ANL-4680

~~SECRET~~ UNCLASSIFIED

~~CONFIDENTIAL~~

Argonne National Laboratory

QUARTERLY REPORT FOR JUNE, JULY, AND AUGUST 1951

PHYSICS DIVISION

CAUTION

This Document Contains Inform[illegible] Affecting the National Defense of the United Sta[illegible] Transmission or the Disclosure of Its Contents [illegible] Manner to an Unauthorized Person is Prohibi[illegible]d May Result in Severe Criminal Penalties Unde[illegible]cable Federal Laws.

RESTRIC[illegible] DATA

This Document Contains Restricted Data as Defined in the Atomic Energy Act of 1946.

UNCLASSIFIED

~~SECRET~~

~~CONFIDENTIAL~~

DECLASSIFIED

DISCLAIMER

This report was prepared as an account of work sponsored by an agency of the United States Government. Neither the United States Government nor any agency Thereof, nor any of their employees, makes any warranty, express or implied, or assumes any legal liability or responsibility for the accuracy, completeness, or usefulness of any information, apparatus, product, or process disclosed, or represents that its use would not infringe privately owned rights. Reference herein to any specific commercial product, process, or service by trade name, trademark, manufacturer, or otherwise does not necessarily constitute or imply its endorsement, recommendation, or favoring by the United States Government or any agency thereof. The views and opinions of authors expressed herein do not necessarily state or reflect those of the United States Government or any agency thereof.

DISCLAIMER

Portions of this document may be illegible in electronic image products. Images are produced from the best available original document.

Photostat Price $ 10.80
Microfilm Price $ 3.90
Available from the
Office of Technical Services
Department of Commerce
Washington 25, D. C.

UNCLASSIFIED

ANL-4680
Physics-Progress Report

ARGONNE NATIONAL LABORATORY
P. O. Box 5207
Chicago 80, Illinois

LEGAL NOTICE

This report was prepared as an account of Government sponsored work. Neither the United States, nor the Commission, nor any person acting on behalf of the Commission:

A. Makes any warranty or representation, express or implied, with respect to the accuracy, completeness, or usefulness of the information contained in this report, or that the use of any information, apparatus, method, or process disclosed in this report may not infringe privately owned rights; or

B. Assumes any liabilities with respect to the use of, or for damages resulting from the use of any information, apparatus, method, or process disclosed in this report.

As used in the above, "person acting on behalf of the Commission" includes any employee or contractor of the Commission to the extent that such employee or contractor prepares, handles or distributes, or provides access to, any information pursuant to his employment or contract with the Commission.

QUARTERLY REPORT FOR

JUNE, JULY AND AUGUST, 1951

PHYSICS DIVISION

Louis A. Turner, Division Director

September 1, 1951

Preceding Quarterlies:

ANL-4552 October-November, 1950
ANL-4602 December 1950, January and February 1951
ANL-4659 March, April, and May 1951

Operated by The University of Chicago

under

Contract W-31-109-eng-38

923 001

CLASSIFICATION CANCELLED
DATE APR 2 1957
For The Atomic Energy Commission
H. R. Carroll
Chief, Declassification Branch

UNCLASSIFIED

THIS PAGE

WAS INTENTIONALLY

LEFT BLANK

TABLE OF CONTENTS

Page

Experimental Nuclear Physics

I. Group #1, Reports by C. O. Muehlhause

1. Resonance and Thermal Neutron Scattering - C. T. Hibdon, C. O. Muehlhause 5

2. Velocity Spectrometer - L. M. Bollinger, S. P. Harris 8

3. Pile Absorption Cross Sections - S. P. Harris, C. O. Muehlhause, H. P. Schroeder, G. E. Thomas 9

4. Internal Conversion of Capture γ-Rays - C. T. Hibdon, C. O. Muehlhause 10

5. Multiplicity of Capture γ-Rays - C. O. Muehlhause 11

6. Neutron Scintillating Crystals - R. Swank, G. E. Thomas 11

II. Group #2, Reports by A. Langsdorf

1. Neutron Transmission Cross Sections in the Kilovolt Region - C. T. Hibdon, A. Langsdorf, J. R. Wallace, R. E. Holland 12

III. Absorption Cross Section of Boron - C. W. Kimball, G. R. Ringo, T. R. Robillard and S. Wexler 29

IV. Crossover Transition in Te^{123} - Bernard Hamermesh, Virginia Hummel 33

V. Results in Nuclear Spectroscopy - W. C. Rutledge 36

VI. Measurement of the Isomeric State of $_{21}Sc^{46}$ (20 Seconds) - S. B. Burson and W. C. Rutledge 41

VII. Product Compounds Formed by Recoil Iodine Atoms in Dilute Solutions of Ethyl Iodide in Benzene and Iodine in Benzene - Frances Mohr and S. Wexler 42

VIII. Yield and Fraction of Positive Gold Recoil Atoms - S. Yosim 48

IX. Conversion Electrons from Capture Gamma-Rays in Gold - S. Yosim 49

923 002

DECLASSIFIED

TABLE OF CONTENTS CONTIN.:

Page

X. Mass Spectroscopy - Reports by M. G. Inghram

1. Fission Yields - Ellis Steinberg, L. E. Glendenin, D. C. Hess, Mark G. Inghram 50

2. Double Beta Radioactive Decay - R. J. Hayden, M. G. Inghram 51

3. Dissociation Energies of Alkali Halide Molecule-Ions - W. A. Chupka 52

4. Argon Geological Age Method - R. J. Hayden, M. G. Inghram 56

Theoretical Physics

XI. Threshold Values of Internal Conversion Coefficients for the K-Shell - B. I. Spinrad and L. B. Keller 58

XII. Thermodynamic Functions on the Generalized Fermi-Thomas Theory - M. K. Brachman 60

XIII. Alphas and Gammas from the Proton Bombardment of Be^9 - D. R. Inglis, R. E. Malm 63

DECLASSIFIED

Experimental Nuclear Physics

I. Group #1 - Reports by C. O. Muehlhause

1. Resonance and Thermal Neutron Scattering (C. T. Hibdon, C. O. Muehlhause)

A. The annular scattering counter was used to measure various thermal and epi-thermal cross sections in a manner described in previous quarterlies. A modification of the method was employed to determine the thermal scattering cross section of U^{235}. This method consisted in making the usual measurements, but both with and without a cadmium tube inside and running the full length of the annular counter. Such a tube removes all thermal scattered neutrons, but it also perturbs the sensitivity of the counter to epi-thermal neutrons. A study was made of the reduction in the sensitivity to epi-thermal neutrons ranging in energy from 0.5 ev (Cd cutoff) to 2 Mev (Ra—α—Be). A reduction factor (0.4246) that was constant to less than 1% was found.

The above property of the scattering counter can be understood by assuming that neutrons (1) are only counted after thermalization, (2) are thermalized after reflection from the paraffin moderator surrounding the BF_3 counting volume. Let: $r(E)$ be the reflection coefficient from the paraffin at energy E, r be the reflection coefficient of thermal neutrons, a be the thermal absorption probability for one passage thru the BF_3 gas. Then:

$$P(\text{no Cd}) = r(E) \cdot a + r(E)(1-a)\, ra + r(E)(1-a)\, r(1-a)\, ra + \ldots$$

$$= r(E) \cdot a/1-r(1-a)$$

$$P(\text{with Cd}) \simeq .8\, r(E) \cdot a$$

$$\frac{P(\text{with Cd})}{P(\text{no Cd})} \simeq .8\left[1-r(1-a)\right]$$

That is, the ratio of counting rates with Cd tube/without Cd tube is independent of neutron energy (above Cd cutoff). In fact, since a may be estimated at $\sim .2$ and r at $\sim .8$ a reduction factor of $\sim .3$ would be expected. This

DECLASSIFIED

value is in fair agreement with the one observed. The effect of fission neutrons may be inferred by subtracting 1/0.4246 times the counting rate with a cadmium tube from the counting rate without the cadmium tube. However, since the fission counting rate is an order of magnitude larger than the counting rate due to thermal scattering, the resulting cross section ($\sigma_{ths}(25) = 9.7$ b) is good only to $\sim$ 20%. The above value is corrected for foil thickness ($\sim$ 6%).

B. Data on scattering and transmission taken by ordinary methods are given in Table I. Cross sections are given in barns. The boron transmission of hafnium scattered resonance neutrons presented in the last quarterly report was re-analysed and a 7.5 ev level assigned to Hf^{178}, and a 6.5 ev level assigned to Hf^{177}. This assignment will be checked in the coming quarter with the resonance region time-of-flight spectrometer. For additional information on hafnium, see sections 3 and 5.

Table I

Element	Compound or Element Used	σ_s Thermal	σ_s Epi-Cd
$_9F^{19}$	CF_2	3.75	3.83
$_{15}P^{31}$	P	4.67	7.54
$_{22}Ti$	Ti	3.96	6.62
$_{90}Th^{232}$	Th	16.9	18.5
$_{92}U^{238}$	U	13.8	19.7

923 005

C. Thermal Scattering by He. (S. P. Harris)

A hydrogen impurity in the helium previously measured was suspected. Spectroscopically pure He was obtained for remeasurement of the thermal scattering cross section. This time a value of 0.78 ± 0.08 b was obtained in better agreement with the one obtained by transmission at Wisconsin.

DECLASSIFIED

Furthermore, it agrees with a value to be expected from the scattering cross sections of the alpha particle nuclei. However, the above value may be lowered still further after analysis of the spectroscopic helium for hydrogen impurity.

D. Absorption Resonance in U^{238} at 7 Ev.

It appears desirable to derive approximate resonance parameters for the 7 ev state in U^{238} inasmuch as this material is important to the A.E.C. and also is very unusual in that it has the lowest cadmium ratio known along with a very small thermal absorption cross section.

$$\Sigma_a = \frac{\pi}{2}\,\sigma_{oa}\,\frac{\Gamma}{E_o} \qquad \sigma_{tha} = \sqrt{40\,E_o}\;\frac{\sigma_{oa}\Gamma^2}{4E_o^2}$$

where $\Sigma_a = 240$ b resonance abs. integral.

$\sigma_{tha} = 2.6$ b thermal abs. cross section

$E_o = 7.0$ ev resonance energy

$\Gamma =$ total width (natural)

$$\sigma_{oa}\Gamma = 1070 \qquad \sigma_{oa}\Gamma^2 = 30.5$$

$$\Gamma = .0285 \text{ ev} \qquad \sigma_{oa} = 37.5 \times 10^3 \text{ b}$$

$$\frac{\Gamma_n}{\Gamma}\left(1 - \frac{\Gamma_n}{\Gamma}\right) = \frac{\sigma_{oa}}{4\pi\lambda_o^2} = \frac{37.5 \times 10^3}{2.60 \times 10^6} \times 7.0 = .101$$

$$\frac{\Gamma_n}{\Gamma} = .114 \qquad \frac{\Gamma_\gamma}{\Gamma} = .886.$$

$$\Gamma_n = .00325 \text{ ev} \qquad \Gamma_\gamma = .0253 \text{ ev}$$

These widths may be compared with the doppler width, Δ:

$$\Delta = 2\sqrt{\log 2 \cdot \frac{mE_o kT}{M}} = .045 \text{ ev at} \sim 300^\circ \text{ K}$$

The effect on the thermal scattering cross section of the 7 ev level is to lower it by $\sim$ 10%. The phase would be normal. Also:

$$\Sigma_s = \frac{\Gamma_n}{\Gamma_\gamma}\,\Sigma_a = .31 \text{ b} \quad \text{resonance scattering integral}$$

This latter value is approximately that given by Table I:

DECLASSIFIED

$$\Sigma_s \simeq 8.4\ (19.7 - 1.1 \times 13.8) = 38\ b$$

2. Velocity Spectrometer (L. M. Bollinger, S. P. Harris)

The burst time at 15,000 rpm was redetermined by detection of γ-rays with a scintillation counter. This yielded a value of 15 μs, which is somewhat larger than that previously used. It has the effect of increasing the inferred energy position of a resonance. For example: As, 44 ev $\rightarrow$ 47 ev; Co, 3.6 kev $\rightarrow$ 6.1 kev.

U^{235} was measured with the chopper with almost exactly the same resolution as that employed by Columbia. Sample thicknesses were either 2.35 gm/cm^2 or 4.70 gm/cm^2. The burst width was 29 μs between 1.4 and 5.0 ev and 15 μs between 4.0 and 2000 ev. Table II lists the transmission dips found by Argonne and Columbia.

Table II

Energy-ev Columbia	Argonne	Comment
6.3	6.3 ± .1	
6.9		Doubtful, Perhaps 28
8.7	8.75 ± .15	
12.0	12.1 ± .3	
13.7	13.7 ± .3	
16.1	15.6 ± .4	
19.0	19.7 ± .5	
24.0	24.0 ± .7	
34.0	34.8 ± 1.0	
50.0	50.7 ± 2.0	
80.0		Also seen as well at Argonne.
120.0		

923 007

DECLASSIFIED

3. Pile Absorption Cross Sections (S. P. Harris, C. O. Muehlhause, H. P. Schroeder, G. E. Thomas)

A 45° phase balancing resistor placed in the detector circuit (cf previous quarterly) had a marked effect in reducing the amplitude of the second harmonic (reduced by a factor of 3). However, it is important to determine its statistical weight relative to the zero-phase resistor. This can be readily accomplished, thereby making the settings of a given sample more sensitive.

One preliminary run was made on a H_2O-D_2O mixture yielding a capture cross section for hydrogen (uncorrected for excess scattering of hydrogen over deuterium) of $\sim$ 0.325 b. R. Ringo's value for the capture cross section of boron (755 b) was used for comparison. A scattering correction $\sim$0.3% upward should be applied. In the coming quarter, this will be determined with greater accuracy and a careful determination of $\sigma_a(H)$ will be made.

Thick samples of enriched Hf^{177} and Hf^{178} were compared with normal Hf. $\sigma(177) \simeq 300 \pm 50$ b, $\sigma(178) \simeq 90 \pm 20$ b. Since the samples were thick it is not clear whether another isotope exists having a large cross section (i.e. > 50 b). The above values are in good agreement with those obtained in a different way (cf sec. 5).

Depleted (30 ppm 25) U_3O_8 was measured in a quartz tube having an inside diameter of $\sim$ 8 mm. A pile cross section of 3.25 b was obtained. However, since U^{238} has the lowest cadmium ratio known a sizable resonance correction ($\sim$20%) had to be made. This was done in the rabbit flux, and the value there converted to the thimble flux via the values for thin gold. The calculation is given below:

Cd R (28 rabbit)	= 7.43	same thickness oxide
Cd R (Au rabbit)	= 4.93	thin

923 008

DECLASSIFIED

Cd R (Au thimble) = 5.83 thim

$$\text{Cd R (28-thimble)} = 1 + \frac{5.83 - 1}{4.93 - 1}(7.43 - 1) = 8.90$$

$$\frac{\text{Sub-Cd}}{\text{epi-Cd}}\ (\text{28-thimble}) = 8.90 - 1 = 7.90$$

$$\frac{\text{Sub-Cd}}{\text{epi-Cd}}\ (1/v\ \text{thimble}) \simeq 131$$

$$\sigma_{pile} = \sigma_{th} + \frac{\sigma_{th}}{7.90} - \frac{\sigma_{th}}{131}$$

$$3.25 = \sigma_{th}(28)\left\{1 + .127 - .008\right\}$$

$$\sigma_{th}(28) = 2.83$$

The 30 ppm of U^{235} reduces the value by $\sim$.02 b; therefore:

$$\sigma_{th}(28) = 2.85$$

The above value assumes σ_{th} (boron) = 740 b and agrees well with the latest value for 28 given by H. Pomerance at Oak Ridge.

4. <u>Internal Conversion of Capture γ-Rays</u> (C. T. Hibdon, C. O. Muehlhause)

Rough values for the K/L ratio for Sm^{150} and Gd^{odd} were obtained on a film densitometer. It is hoped that the following values can be wrong by no more than a factor of 2, but more careful work is planned to insure this. An uncertainty of $\lesssim$ 30% is needed to distinguish between M1 and E2 transitions. The K/L ratios obtained were $\sim$4, thus indicating E2 transitions for both γ-rays in a single even-even isotope. Since these γ-rays are presumed to be just above ground, the probable level scheme is as follows:

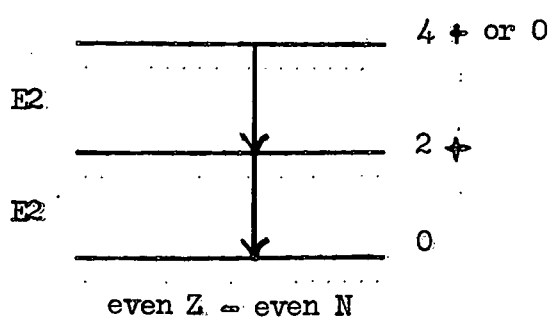

DECLASSIFIED

5. Multiplicity of Capture γ-Rays. (C. O. Muehlhause)

A study of the multiplicity and capture cross sections of Hf^{177}, Hf^{178} and normal Hf was made with a pair of scintillation counters in coincidence. A careful background analysis was made as outlined in older quarterlies and Phys. Rev. 79, 277 (1950). Table III lists the results obtained.

Table III

Material	$\overline{\nu_\gamma}$	σ_a
Hf^{177}	$4.1 \pm .2$	310 ± 50
Hf^{178}	$3.5 \pm .2$	70 ± 20
Hf^{normal}	$3.6 \pm .2$	110 ± 10
Sm^{149}	$5.6 \pm .2$	
Cd^{113}	$4.3 \pm .2$	

The above figures on hafnium would indicate the existence of another important absorbing isotope (e.g. 179), since not all of the absorption in normal hafnium is accounted for. If Hf^{177} is associated with the 1.0 and 6.5 ev resonance, and Hf^{178} is associated with the 7.5 ev resonance, the resonance at 2.3 ev is still unassigned.

6. Neutron Scintillating Crystals (R. Swank, G. E. Thomas)

Additional Tl activated LiI crystals have been grown with an improvement in pulse height of $\sim$2.5 (cf previous quarterly). It appears very easy to grow large crystals of this material. One or more crystals totaling $\sim$ 15 lbs would make a marked improvement in resonance neutron detection. The growth of such crystals seems feasible. Sn activated LiI has also been grown. It has comparable characteristics. However, the fluorscent radiation from Tl is more suitable (u.v. - blue) for 5819 photomultiplier tubes than is the radiation from Sn (green).

923 010

DECLASSIFIED

II. Group #2 - Reports by A. Langsdorf

1. Neutron Transmission Cross Sections in the Kilovolt Region (C. T. Hibdon, A. Langsdorf, J. R. Wallace, R. E. Holland)

Neutron transmission cross sections have been measured with about 2 kev resolution in the energy range from 2 kev to 25 kev, and to higher energies in some cases. The neutrons, produced by the $Li^7(p,n)Be^7$ reaction with a van de Graaf generator, were detected by a highly efficient (~15%) bank of boron trifluoride filled proportional counters placed to detect neutrons emitted at an angle of 120° from the proton beam direction. Measurements at the lower energies were made possible by a collimator and shield around the counters, which reduced background, and by the high efficiency obtained by many counters embedded in an array in a paraffin moderator. Resonances were observed in Na, Ti, V, Mn, Fe, Co, and Ni.

Introduction

Hitherto, a gap has existed in the data on neutron cross sections between the lowest energies that could be satisfactorily measured with the electrostatic generator (about 15 kev) and the highest energies for which velocity spectrometers have adequate resolution (about 3 kev). Several groups[1-4] have been developing methods of increasing the upper energy limit of time of flight spectrometers and undoubtedly in the near future improved resolution will be obtained.

The lower energy limit to the electrostatic generator technique as developed by Barschall et al[5] has been determined by the rapid fall in neutron yield of very low energy neutrons and the large background counting

1. Nuclear Sci. Abst. 5, 636 August 15, 1951. (Refers to CUD-65, Sec. 1; DR-1578)
2. W. Selove, Phys. Rev. 76, 187 (1949).
3. Hibdon, Muehlhause, Selove and Woolf, Phys. Rev. 77, 730 (1950).
4. A. W. Merrison and E. R. Wiblin, Nature 167, 346 (1951).
5. Barschall, Bockelman and Seagondollar, Phys. Rev. 73, 659 (1948).

DECLASSIFIED

rate (for the $Li^7(p,n)Be^7$ reaction; no other reaction has been used so successfully, as yet, for this low energy neutron work). In this work to be reported, a new detection scheme has been employed in which a massive shield reduces the background counting rate and the large group of boron trifluoride proportional counters embedded in paraffin increases the counting efficiency to overcome the decline in yield of low energy neutrons. This equipment has been briefly described[6] and will be more fully described in a later publication elsewhere. Figure 1 shows the essence of the device.

Procedure

The collimator and shield, Figure 1, was set up with its axis at 119.6° to the proton beam direction, as determined by triangulation with a transit. Transmission samples were placed immediately in front of the collimator hole entrance. No corrections for scattering-in by the scattering sample are necessary in this arrangement. Neutron flux monitoring was achieved by a standard boron-trifluoride "long counter"[7] placed in the neutron flux along a line extended from the proton beam direction. Presence or absence of a transmission sample does not appreciably disturb this monitor since scattering by the face of the shield is already complete and the sample scarcely perturbs the scattering equilibrium. Measurements were made with and without the transmission samples and with and without a paraffin plug 2" in diameter by 5½" long placed at the scattering sample position inside the counter assembly in the collimated beam. Measurements without the paraffin plug are the background measurements. This technique of background measurement differs from the prior method involving use of a paraffin cone[5,8]

6. A. Langsdorf, Jr., Phys. Rev. 80, 132 (1950).
7. A. O. Hanson, J. L. McKibben, Phys. Rev. 72, 673 (1947).
8. J. M. Blair and J. R. Wallace, Phys. Rev. 79, 28 (1950).

DECLASSIFIED

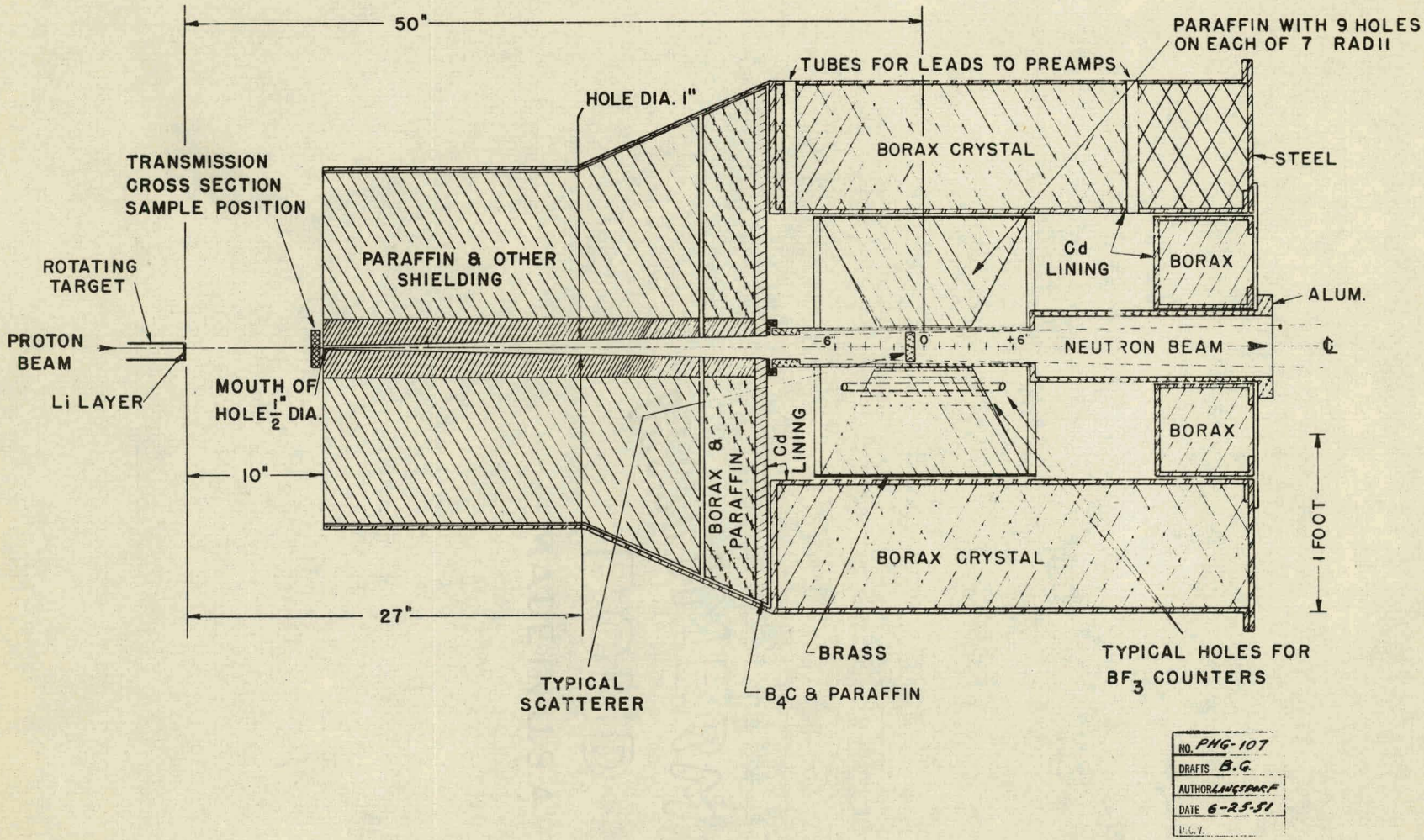

Fig. 1

Collimator and Shield with Neutron Counter Assembly Inside the Shield. In this work the collimator was placed at 119.6° to the proton beam direction instead of at 0° as shown. The paraffin plug 2" dia. x $5\frac{1}{2}$" long was located similarly to the "typical scatterer" in the cut. The solid angle subtended by the collimator at the neutron source is .001 steradian.

923 013

and is probably more reliable and less likely to be disturbed by systematic errors. The paraffin plug when in position was located at a point at which the counting rate was a maximum (except in some of the earlier exploratory data.)

The lithium targets were evaporated onto the tantalum end cap of the rotating target and the thickness was controlled by observing the neutron yield during evaporation and then measured by the rise curve, as described by Taschek.[9] A typical rise curve is shown at the left side of Fig. 2. The rise curve was usually rerun before and after each day's work and a new target prepared if the old one was found to be too thick. Proton energies were measured relative to the Li(p,n) threshold at 1.882 Mev and neutron energies calculated as described by Hanson et al.[10] Neutron counting rates near the 120° threshold are shown at the right side of Fig. 2. In the accompanying table, a typical measurement and calculation is shown.

Energy Resolution

The best measure of the overall energy resolution is attained by observation of the measured widths of the sharpest observed resonances, which are about 1.5 to 2 kev full width at half-maximum. Part of the energy spread is due to the finite angular spread of neutrons accepted by the detector, namely, ± 1° from the mean angle of 119.6°. This introduces a spread of[10] about ± 500 ev which is small compared to the overall resolution observed. The spread in energy due to target thickness measured as described above, proton beam energy spread, and beam energy fluctuations together are about double the observed neutron energy resolution, hence, must be about 3 to 4 kev. The exact relation depends upon energy.[10] Since targets about 2 kev thick were used, the proton beam energy spread plus fluctuations is not over about 2.5 to 3.5 kev.

9. R. F. Taschek and A. Hemmendinger, Phys. Rev. 74, 373 (1948).
10. A. O. Hanson, R. F. Taschek, J. H. Williams, Rev. Mod. Phys. 21, 635 (1949).

DECLASSIFIED

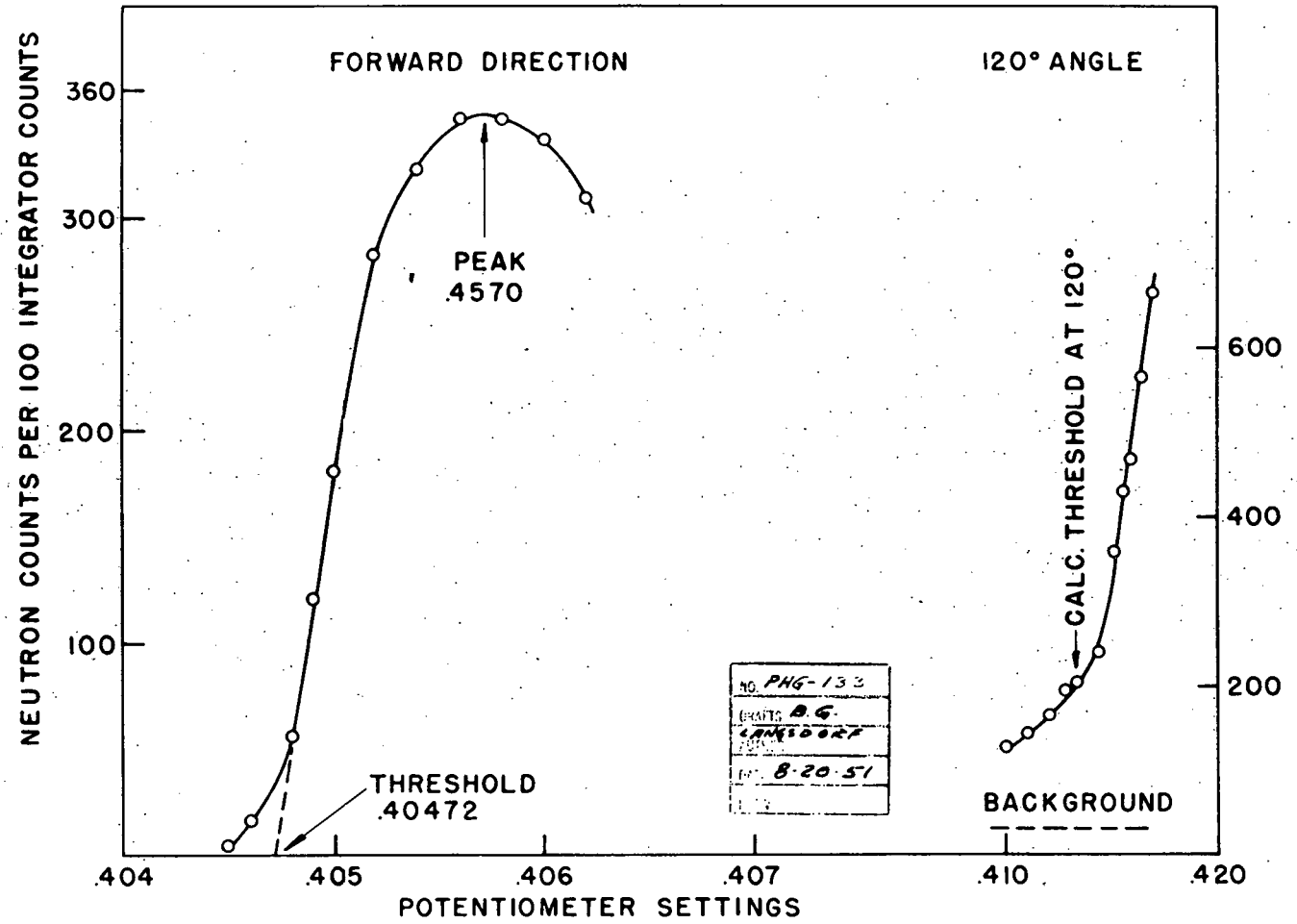

Fig. 2

At left: typical target thickness and threshold determination data. At right: neutron counting rate at 120° to proton beam using collimator-detector, in the region from just below to just above the threshold for appearance of neutrons at this angle. The point marked threshold at 120° is calculated from the threshold point determined by the graph at the left. The tail of the counting rate curve below threshold at 120° was higher here than it should have been because a small air blower accidentally was in the flux of neutrons at 60° to the proton beam and in the line of sight of the collimator so neutrons were back-scattered into the detector.

DECLASSIFIED

923 015

Typical Data

Neutron threshold observed at potentiometer setting 0.40420 volt. Potentiometer setting for this data 0.41547 volt. Lithium target thickness by rise curve, 1.4 kev. Peak neutron energy at 119.6° calculated 2 kev; mean energy 1.7 kev. Time for each 40,000 monitor counts about 320 seconds. Beam current approximately 10 microamperes.

Transmission Sample	Detector Scatterer	Monitor Counts	Detector Counts	Reduced* Detector Counts	Net Counts	I_o/I	Atoms/ Cm^2 $x10^{-24}$	σ_t Calc. Barns
Open-beam (I_o)	In	40003	2897	2897				
	Out	40360	305	302	2595			
Na	In	39670	2483	2504				
	Out	39968	292	292	2212	1.173	.0165	9.5±2
Mn	In	40984	1301	1270				
				292 ‡	978	2.65	.0510	19±1

* Corrected to 40,000 monitor counts.
‡ Background assumed same as measured for Na, error in this assumption is negligible.

DECLASSIFIED

Results

Iron. The iron sample used was "Puron" brand of specially pure iron made by Westinghouse Electric Co. Spectrographic analysis showed no impurity sufficient to interfere in these measurements. Figure 3 presents the results. The resonance observed at 8.5 kev was expected to be present, as prior unpublished resonance overlap data obtained by the annular chamber technique using a pile beam and a vanadium detector had shown overlapping resonances. The resonance overlap method has been described by Hibdon and Muehlhause.[11] The results on V presented in Fig. 6 confirm the overlap of resonances at about 8 kev. There may be a weak resonance in Fe at 16 kev but the data are insufficient to establish it. The 8.5 kev resonance is certainly in one of the iron isotopes of minor abundance.

Nickel. The nickel sample contained somewhat under one percent cobalt impurity, and less of other known impurities. Resonance peaks are evident in the data (Figure 4) at 4.5 and 17 kev and possibly a weaker resonance at 30 kev. The 17 kev resonance is undoubtedly the one reported by Barschall et al[5] at 15 kev. The lower resonance may be the one observed in the 4 kev region by the Columbia University group.[12] At this laboratory, strong resonance overlapping has been observed between nickel and sodium and also nickel and vanadium (not published). One may conclude that the nickel 4.5 kev resonance, shows some overlapping with the 2.8 kev resonance in Na and the 7 kev resonance in V.

Titanium. Figure 5 presents the results for several separate runs on this element. Resonances are indicated at 19 and 23 kev with a narrow minimum near 22 kev which was best resolved with a thin sample. The largest known impurity in the titanium is 0.1 percent of manganese. The fall in cross section from 2 to 6 kev suggests there may be a resonance below 2 kev. Results from annular chamber measurements using a vanadium detector indicated resonance

11. C. T. Hibdon and C. O. Muehlhause, Phys. Rev. 76, 100 (1949); C. T. Hibdon, Phys. Rev. 79, 747 (1950).
12. W. W. Havens, Jr. and L. J. Rainwater, Phys. Rev. 75, 1296 (1949).

DECLASSIFIED

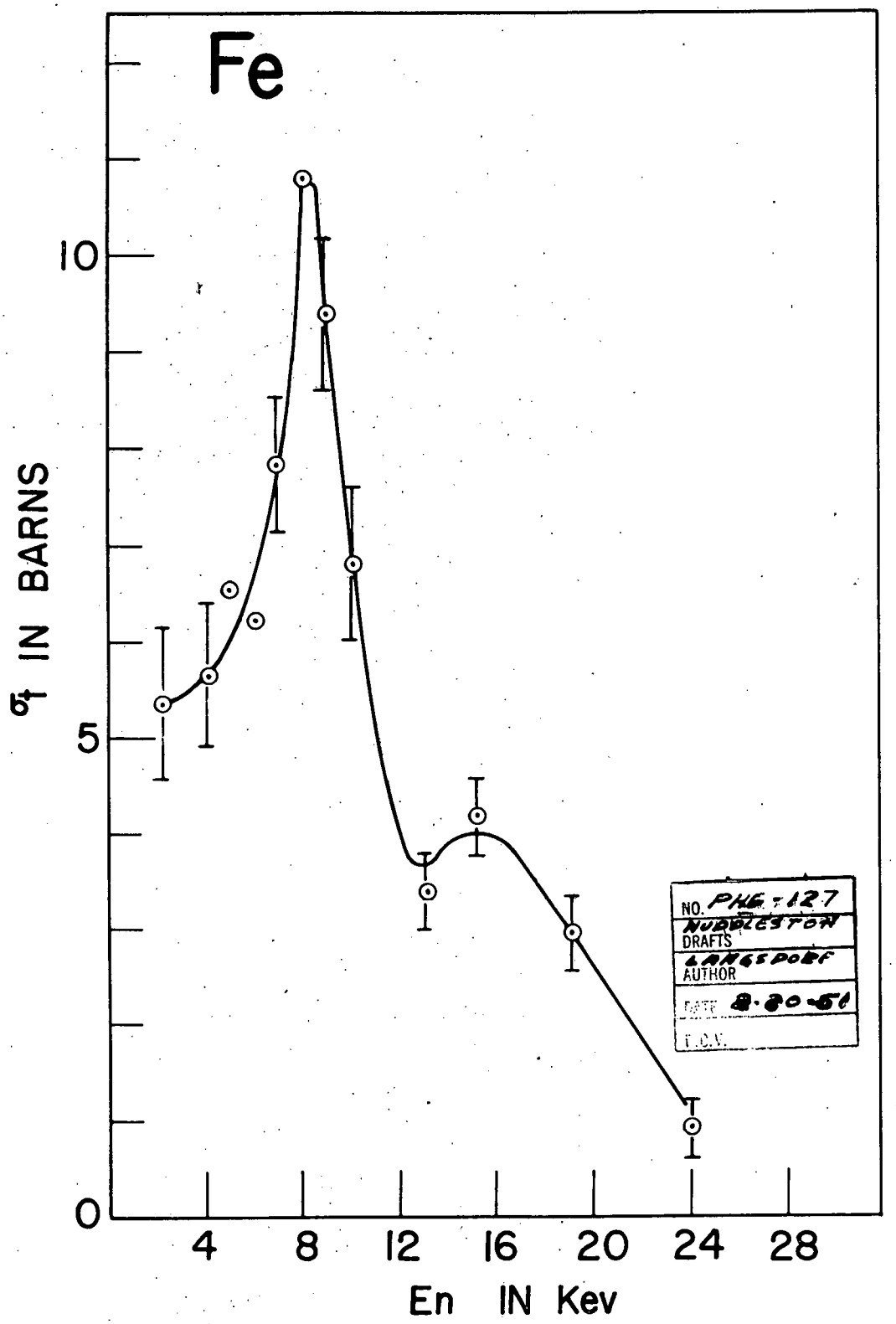

Fig. 3

Transmission Cross Section of Iron. Thickness 0.1613 x 10^{24} atoms/cm^2. Li target thickness 2.9 kev.

923 018

DECLASSIFIED

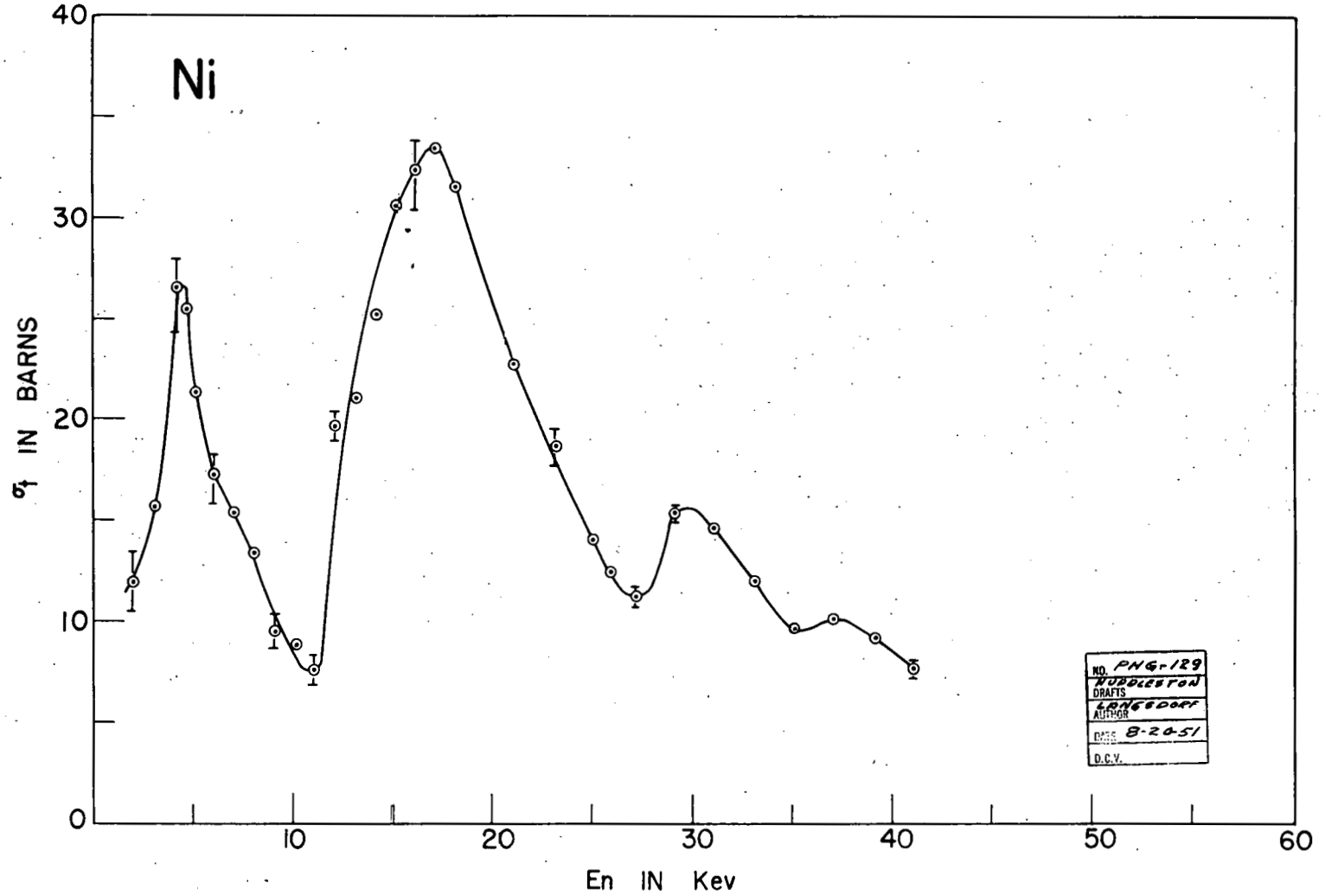

Fig. 4

Transmission Cross Section of Nickel. Thickness 0.0698 x 10^{24} atoms/cm^2. Li target thickness: 3.0 kev to 6 kev neutron energy; 3.5 kev, 7 to 24 kev neutron energy; 2.4 kev, 26 to 41 kev neutron energy. Probable errors of all points similar to those of nearby points for which it is shown.

923 019

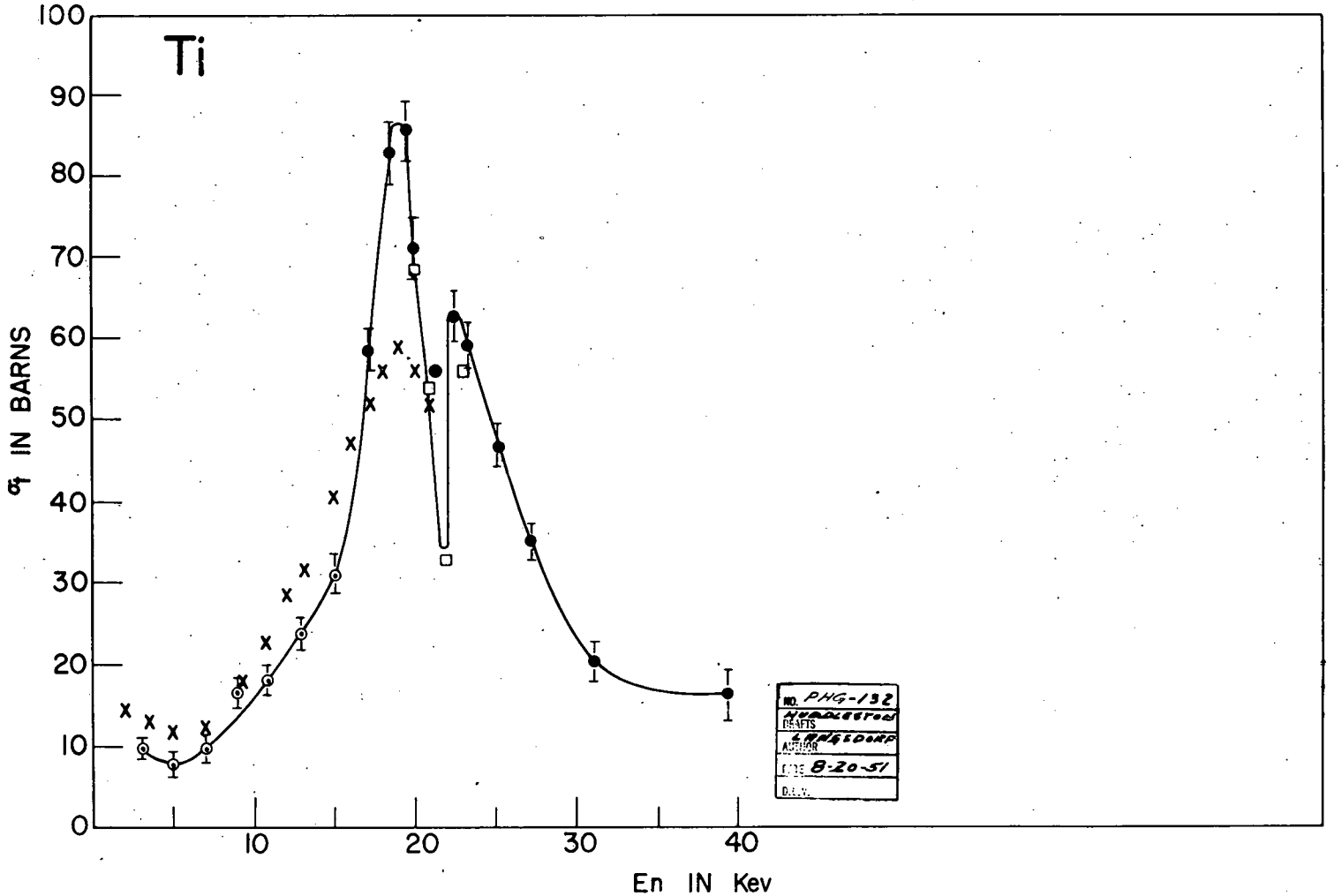

Fig. 5

Transmission Cross Section of Titanium. Open circles: titanium thickness 0.1037 atoms/cm^2, lithium target 3.7 kev. Solid circles: titanium thickness 0.011 x 10^{24} atoms/cm^2, lithium target thickness 3.7 kev. Crosses: titanium sample .0343 x 10^{24} atoms/cm^2, lithium target thickness 3.1 kev. Squares: titanium sample 0.011 x 10^{24} atoms/cm^2, lithium thickness 3.1 kev. Probable errors of all points about the same as for those indicated.

UNCLASSIFIED

623 020

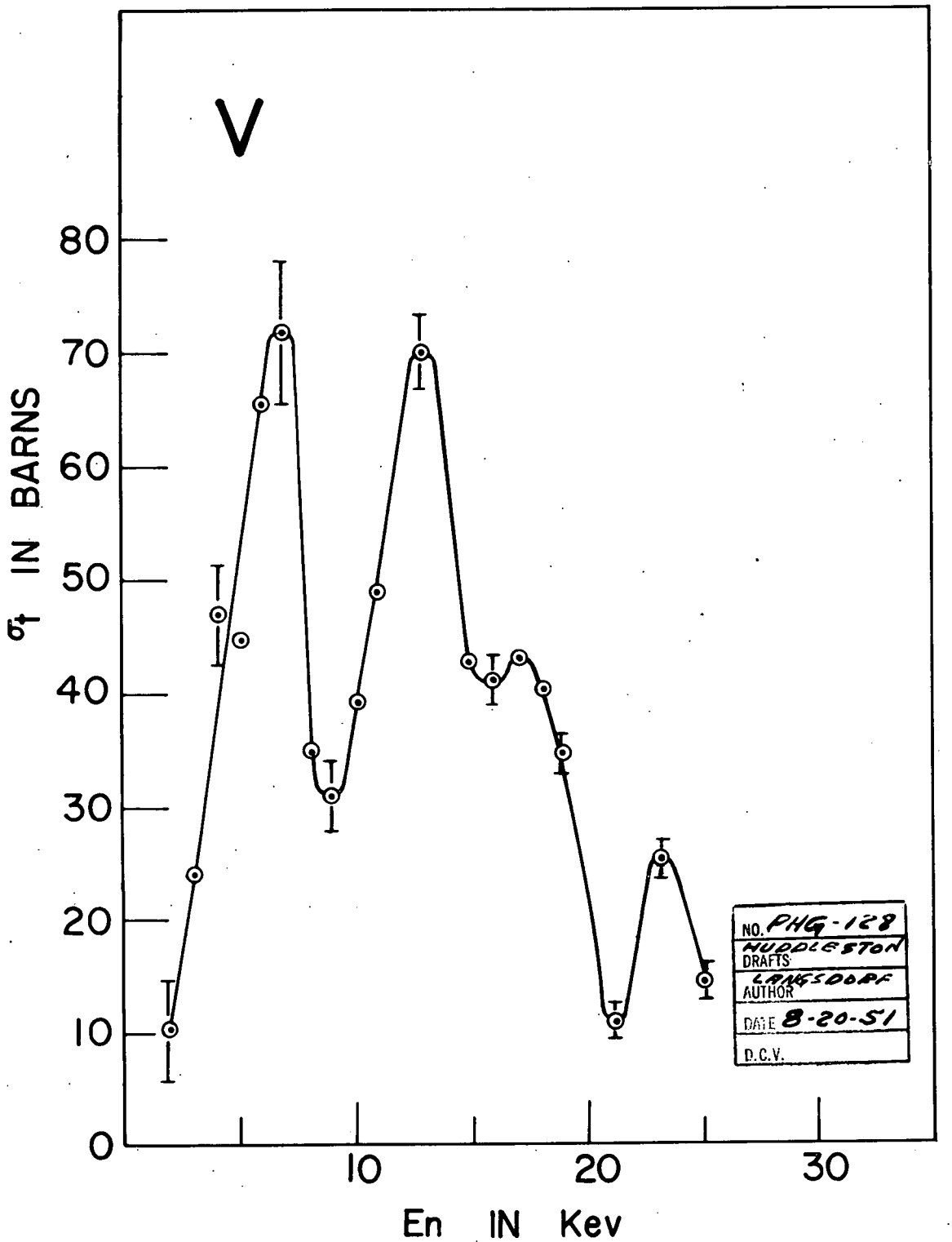

Fig. 6

Transmission Cross Section of Vanadium. Thickness .0228 x 10^{24} atoms/cm^2, lithium target thickness 1.6 kev to 11 kev neutron energy, 2.6 kev above.

DECLASSIFIED

overlapping with titanium, which, comparing Fig. 5 and 6, may be due to overlap of the 17 kev resonance in V with the 19 kev resonance in Ti.

Cobalt. In Fig. 7 results of three runs on cobalt are presented. Resonances are indicated at 5.5 and 29.5 kev and a poorly resolved resonance at 8 kev is probably present. Insufficient data was obtained to determine higher energy resonances which may lie in the vicinity of 53, 78, and 88 kev. The cobalt samples contained major impurities of Cr 0.5%, Fe 1%, Ni 0.5%. Prior unpublished resonance overlap observations with Na and V detectors are explained by the overlap of the 5.5 kev Co resonance with the 2.8 kev Na resonance (Fig. 8) and the 7 kev V resonance (Fig. 6). Time of flight spectrometer data from Columbia University[1] and Argonne National Laboratory (unpublished) had indicated a resonance in the 3 to 10 kev region which is undoubtedly the doublet observed here at 5.5 and 8 kev.

Vanadium The resonance overlapping of vanadium and cobalt which had been observed previously led us to measure V and Co both by this new technique. The results for V are shown in Fig. 6. Strong resonances are apparent at 7 kev and 13 kev, and a partially resolved resonance at 17 kev. There is probably a smaller resonance near 23 kev. The major impurity in the vanadium sample is 0.5% carbon. Time of flight spectrometer data had indicated a resonance at 3300 ev[13] which has been recalculated to lie at about 6 kev. This is undoubtedly the resonance observed here at 7 kev.

Sodium The existence of a resonance in sodium was first discovered[3] by the unexpected resonance overlap effect found with a manganese detector using the annular scattering chamber. The fact that this overlap was related to resonances near 3 kev was determined by neutron time of flight spectrometer measurements. The present work confirms this earlier work, and has better resolution, especially on the high energy side of the resonances. The sodium

13. S. P. Harris, Phys. Rev. 83, 235 (1951).

DECLASSIFIED

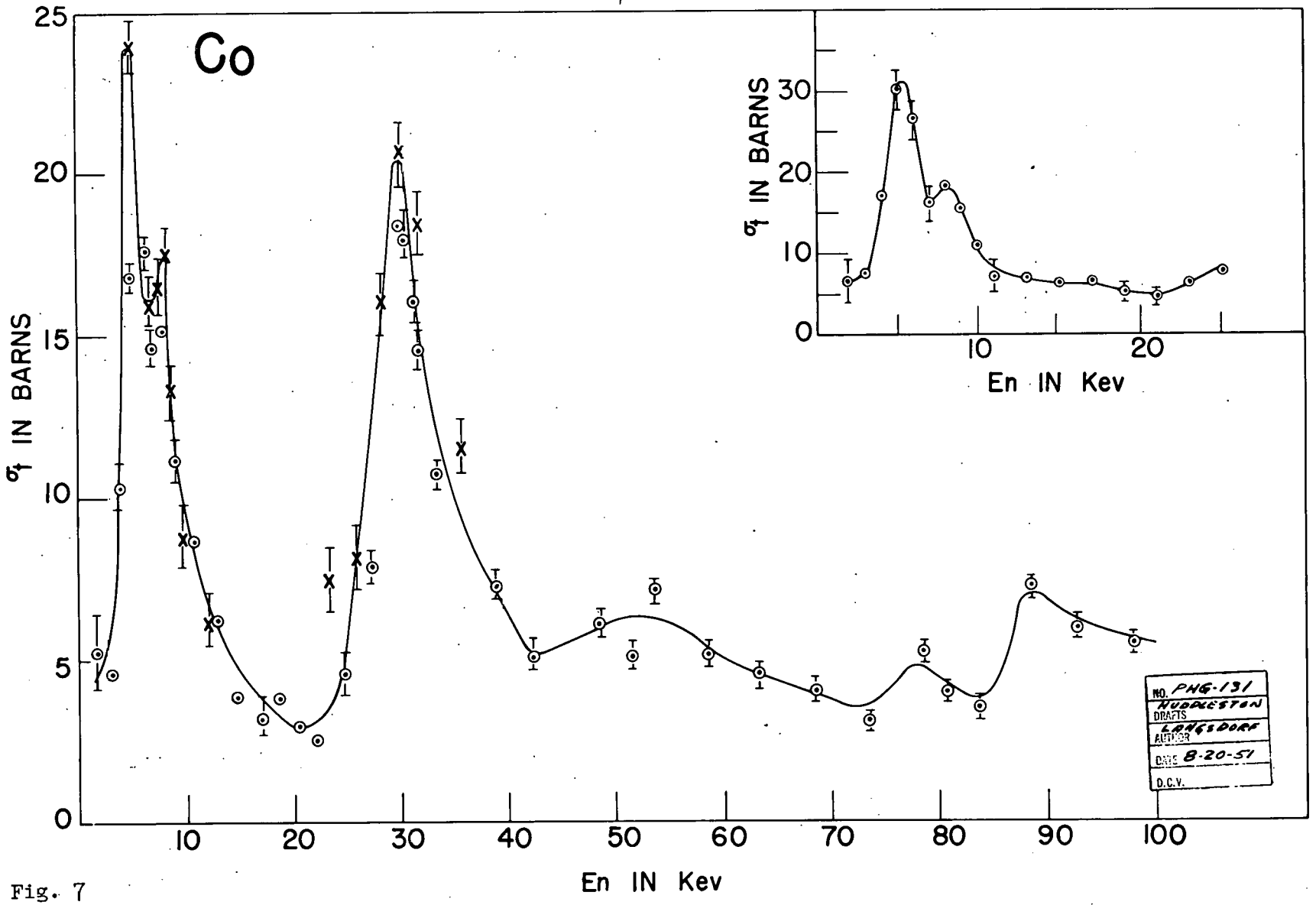

Fig. 7

Transmission Cross Section of Cobalt. Large graph, open circles: Cobalt thickness 0.0822 x 10^{24} atoms/cm^2, lithium thickness 4.4 kev; Crosses: Cobalt thickness 0.0419 x 10^{24} atoms/cm^2; lithium thickness 1.4 to 17.5 and 4.6 above kev. Inset graph at upper right: Cobalt thickness $\sim$ .02097 x 10^{24} atoms/cm^2; lithium thickness 1.6 kev to 11 kev neutron energy, 2.6 kev above. Probable error of all points about the same as for nearby points for which it is shown.

DECLASSIFIED

023 023

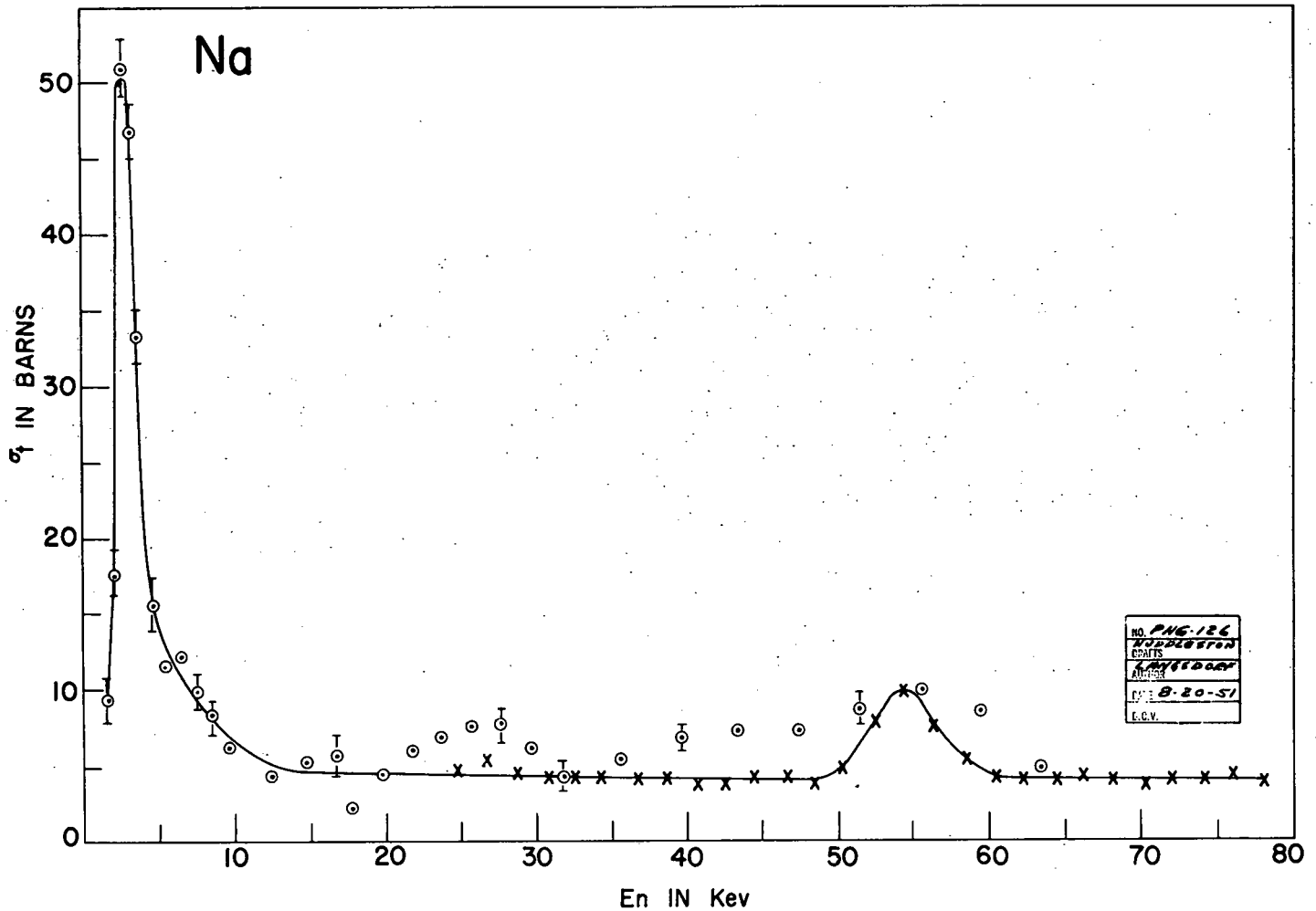

Fig. 8

Transmission Cross Section of Sodium. Circles: sodium thickness .0165 x 10^{24} atoms/cm^2, lithium target thickness 1.4 kev to 17.5 kev neutron energy, 4.6 kev above. Crosses: sodium thickness .0666 x 10^{24} atoms/cm^2, lithium thickness 7.1 kev. Probable error of all circled points similar to those for which indicated, for crosses about the size of the cross.

DECLASSIFIED
523 024

data is shown in Fig. 8. The first sodium sample used to obtain clearer results near 2.8 kev was too thin at higher energies. Better data above 25 kev was later obtained using a thicker sample. Another resonance occurs at 55 kev which is undoubtedly the same one observed by Adair et al[14] at 60 kev.

The sodium used was ordinary commercial metal sealed in a cylinder with one mil thick steel diaphragm covers on the ends. It was not analysed chemically.

Manganese. The results for manganese are shown in Fig. 9. In addition to the resonance mentioned above, at 2.8 kev, others are clearly shown at 8, 23, and 38 kev. Less pronounced ones probably occur in the vicinity of 60, 67, and 78 kev.

The manganese contained about 1% iron, all other impurities less than .01% by spectrographic analysis.

Discussion

The most important feature of the work reported is the presentation of a method for extending the electrostatic generator techniques downward in neutron energy range to 2 kev or even lower. The new method of detecting neutrons with a highly efficient shielded detector is responsible for this extension in range. It is a fortunate feature of the technique of measurement at "back-angles" (e.g., at 120° to the proton beam direction as here employed) that the neutron energy resolution is about twice the resolution in energy of the proton beam and lithium target thickness. This circumstance leads us to believe that with the use of a new 40" radius electrostatic analyser now under construction similar to the one at the University of Wisconsin,[15] sufficient resolution will be attained to permit measurements with about 1 kev resolution down to as low as 1 kev neutron energy before running into insuperable difficulties.

523 025

14. Adair, Barschall, Bockelman, and Sala, Phys. Rev. 75, 1124 (1949).
15. R. E. Warren, J. L. Powell, R. G. Herb, Rev. Sci. Inst. 18, 559 (1947).

DECLASSIFIED

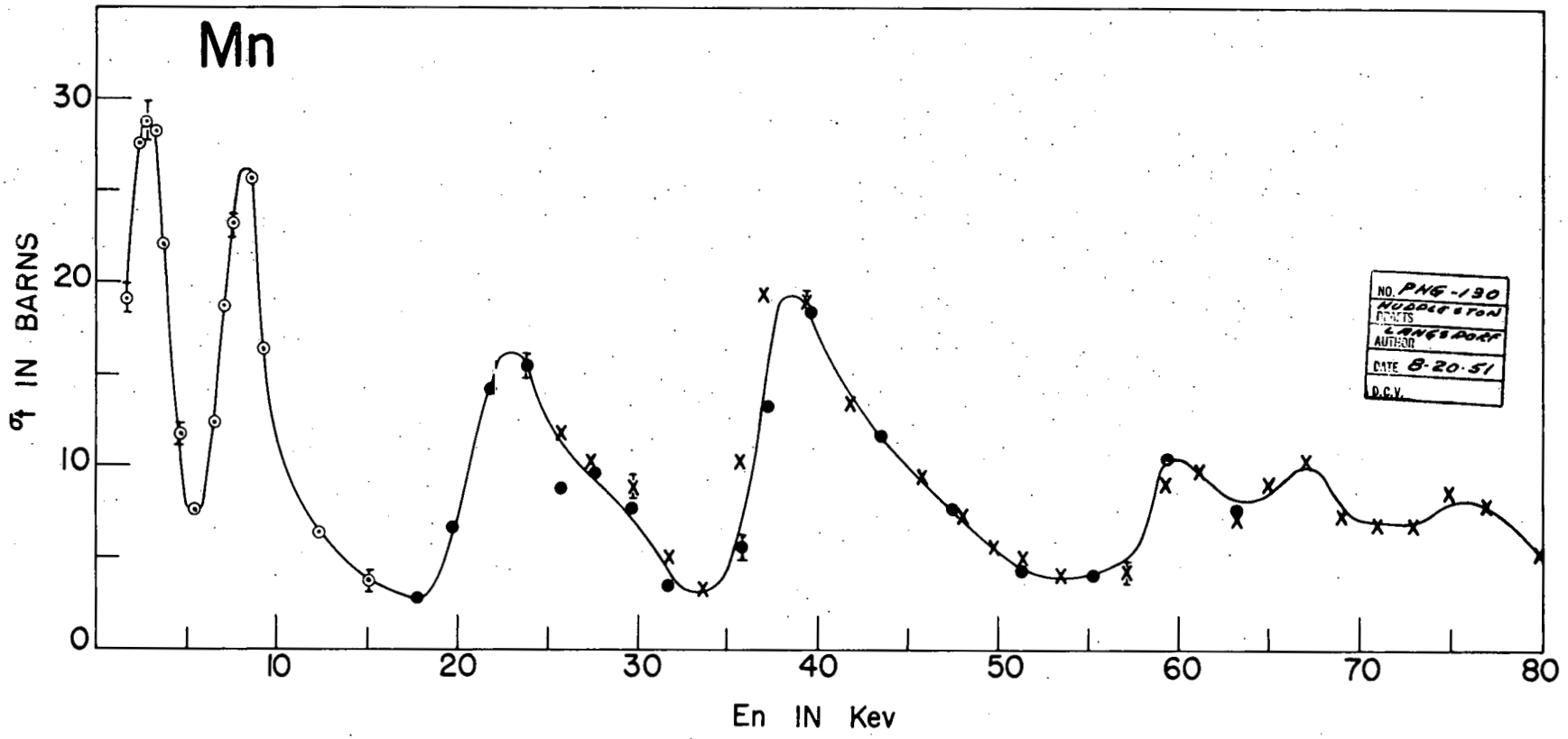

Fig. 9

Transmission Cross Section of Manganese. Manganese thickness 0.051 x 10^{24} atoms/cm^2. Open circles: lithium target thickness 1.4 kev; solid circles: lithium thickness 4.6 kev; crosses: lithium thickness 7.1 kev. Probable errors of all points about the same as for those indicated.

DECLASSIFIED
923 026

It will also be possible to apply resonance self-detection and resonance overlap techniques in neutron cross section measurements with this equipment. If the scattering sample position inside the paraffin and counter assembly is occupied by some element under investigation instead of the paraffin plug used in the measurements reported here, additional data can be obtained by transmission measurements concerning resonance widths and peak cross sections. This technique will permit determination of resonance properties with resolution better than that afforded by the actual neutron beam energy spread.

It may also be pointed out that this equipment permits transmission cross section measurements with relatively small samples of rare elements or separated isotopes. Since the neutron source spot can be held to a region about 1/16" diameter and the angular spread of the detector is only 2 degrees, many materials might be measured with fair accuracy in the region of a resonance with a sample (about 5/16" diameter) weighing about one gram.

The closing of the gap in knowledge of neutron cross sections between 2 and 15 kev will now permit more accurate calculations of interesting thermal neutron properties of many elements, including such properties as the phase of scattering and the coherent and incoherent scattering amplitudes.

DECLASSIFIED

III. Absorption Cross Section of Boron (C. W. Kimball, G. R. Ringo, T. R. Robillard and S. Wexler)

Most measurements of cross sections for absorption of thermal neutrons are made by comparison with a standard such as boron or gold. Since these cross sections are of obvious technological importance and the absorption cross section of hydrogen is of interest in nuclear theory, it was decided to make a careful measurement of the absorption cross section of a reference standard. This reference cross section must be measured absolutely, which means by transmission (correcting for scattering) since the alternative schemes bring in all the difficulties of absolute neutron and absolute alpha or beta counting. The reference standard should have a large ratio of absorption to scattering cross section, be a 1/v absorber to quite high energies and be mono-isotopic (so that it will be the same from sample to sample). Unfortunately, no naturally occurring material meets these requirements and one of them had to be abandoned. It was felt that the last requirement was of the least fundamental importance and could be partially circumvented by mixing a large batch and using only material from this one batch as a standard, perhaps later measuring a secondary standard which was mono-isotopic. Accordingly, boron was picked for the standard as it meets the first two requirements very well.

Boric acid was ignited to B_2O_3 and dissolved in heavy water. The solution containing 30.20 mg of B_2O_3 per gm of solution was placed in a cell with glass windows which was kept at about 42° C to avoid any danger of the B_2O_3 precipitating. An identical cell was filled with pure D_2O and also kept at 42° C. The transmissions of these two cells were measured in two velocity ranges, one near 1000 m/sec, the other near 2000 m/sec using the time-of-flight velocity selector for thermal neutrons. The cross section for

DECLASSIFIED

boron at 2200 m/sec was calculated from the difference in the transmissions of the two cells and the nominal velocity calibration of the velocity selector. This cross section, column 4 of Table IV, was then corrected for the following factors.

1. True velocity. This was determined by location of the sharp rise in the Be cross section as the neutron wavelength becomes short enough to diffract from the longest spacing in the Be crystal. This occurs at 3.95 Å and results in a change of 20% in Be cross section per percent change in velocity in the transition region. This served to calibrate the 1000 m/sec group directly. The 2000 m/sec group was obtained by simply doubling the distance from chopper to counter which should have left the optical-mechanical and electrical delays unchanged, hence, have given twice the velocity in any given channel.

2. Counter dead time. This was determined by measuring the ratio of counts in the first and last channels of the velocity selector when it was set on a certain region of the thermal spectrum and the total intensity changed by narrowing a slit of constant height.

3. Scattering. The scattering cross section[1,2] of $BO_{1.5}$ (8.8 barns) was subtracted and the scattering cross section[2] of the D_2O displaced by the boric oxide was added.

4. Concentration. This was checked by chemical analyses by R. W. Bane's group of the Chemistry Division. In general, the analyses agreed with the calculated concentration from the weights of materials added to the mixture. These concentrations had to be corrected for the densities at

1. G. T. Hibdon, ANL-4552, p. 6 (Dec. 8, 1950).
2. R. K. Adair, Rev. Mod. Phys. 22, 249 (1950).

DECLASSIFIED

42° C. These densities were not available when the first cross sections were calculated, hence, this factor appears as a correction.

The following corrections were considered and found negligible.

5. Empty cell transmission. These were found to be identical for the two cells both before filling and after emptying.

6. Scattering in. Only about 1 neutron in 10,000 would have been scattered in, in the worst geometry unless there were a small angle scattering which has never been seen in liquids. In any event, the cross sections do not seem to vary with geometry.

7. Finite width of velocity selector channels.

The corrections and the corrected values of the cross section are shown in Table I. The average value with a somewhat subjective weighting of the values is 755 ± 1.5 barns at 2200 m/sec. The probable error comes from the fluctuations among the groups, The cross section is somewhat higher than the previously reported values, 700,[3] 707,[4] 732,[5] 743,[6] but this is not necessarily an argument against it as a large share of this difference could be accounted for by variations in isotopic abundance and this value is intended to apply only to the particular sample tested. It is intended, however, to get at least a rough check by comparison of this boron with gold by the danger coefficient method in CP-2. A secondary standard such as iron will also be measured.

---

3. Fermi, Marshall and Marshall, Phys. Rev. 72, 193 (1947).
4. Bacher et al, Phys. Rev. 69, 443 (1946).
5. Sutton et al, Phys. Rev. 71, 272 (1947).
6. Rainwater et al, Phys. Rev. 70, 136 (1946).

923 030

DECLASSIFIED

Table 1

Boron Cross Section Measurements

Group	Velocity Selector[1] Angle Setting	Counter Distance	Preliminary σ[2]	Velocity Correction	Dead Time Correction	Scattering Correction	Concentration Correction	Final σ[2]
1	104.5°	150 cm	735.4 ± 1.9 barns	1.0045	1.0143	1.0022	1.0042	754.1 ± 1.9
2	104.5°	150	739.2 ± 2.5	.9993	1.0143	1.0022	1.0042	754.1 ± 2.5
3	64.5°	244	740.0 ± 3.0	1.0070	1.0056	1.0022	1.0042	754.2 ± 3.0
4	64.5°	488	741.1 ± 2.0	1.0048	1.0135	1.0005	1.0042	758.4 ± 2.0
							Weighted average	755 ± 1.5

(1) All measurements were made with a rotor speed of 60 rps.

(2) The errors given are based on fluctuations among the runs in each group and, in the final average, among the groups.

IV. Crossover Transition in Te^{123} (Bernard Hamermesh and Virginia Hummel)

The disintegration scheme[1] of Te^{123} (100 days) consists of an 88.5 kev gamma ray followed by a 159 kev line. The shell model predicts an $s_{\frac{1}{2}}$ ground state with $d_{3/2}$ and $h_{11/2}$ as the first excited states. If the order of levels is $s_{\frac{1}{2}}$, $d_{3/2}$, $h_{11/2}$, then the 88.5 kev line is due to an M4 transition and the 159 kev line is due to a M1 transition. The crossover, i.e. $h_{11/2} \rightarrow s_{\frac{1}{2}}$ (248 kev) is an E5 transition. The validity[2,3] of this level assignment has been demonstrated previously. Weisskopf[4,5] theory predicts that the crossover ratio, i.e. $\frac{\lambda_{E5}}{\lambda_{M4}}$ is equal to 7×10^{-2}. The present experiment was performed to check this value.

A sample of highly enriched Te^{122} was irradiated in the Argonne heavy water-moderated reactor. The gamma rays emitted were then examined with a NaI crystal and photomultiplier. The pulses were analyzed with a 20-channel pulse height discriminator. The source was first placed so that the counting rate at 159 kev could be determined accurately. The source was then moved as close to the crystal as possible so that the discriminator still gave reliable results and the counting rate at the crossover energy was as high as possible. The results were then normalized.

The pulse height distributions corrected for background are shown in Figure 10. (III). The normalization factor is 7.7. It may be seen that there is no evidence of a peak at 248 kev. The counting rates at 51, 53 and 55 volts are nearly the same. The difference in rate between 53 and 51 or 55 volts is 0 ± 3 scales of ten. However, it is possible to set a very conservative upper limit on the value of the crossover ratio from the

1. N.B.S. Circular 499
2. M. Goldhaber and A. W. Sunyar, Phys. Rev. 83, Aug. issue (1951).
3. S. Moszkowski, Phys. Rev. 83, Aug. issue (1951).
4. V. F. Weisskopf and J. Blatt, privately circulated chapter from forthcoming book on "Nuclear Theory".
5. R. D. Hill, Phys. Rev. 81, 470 (1951).

DECLASSIFIED

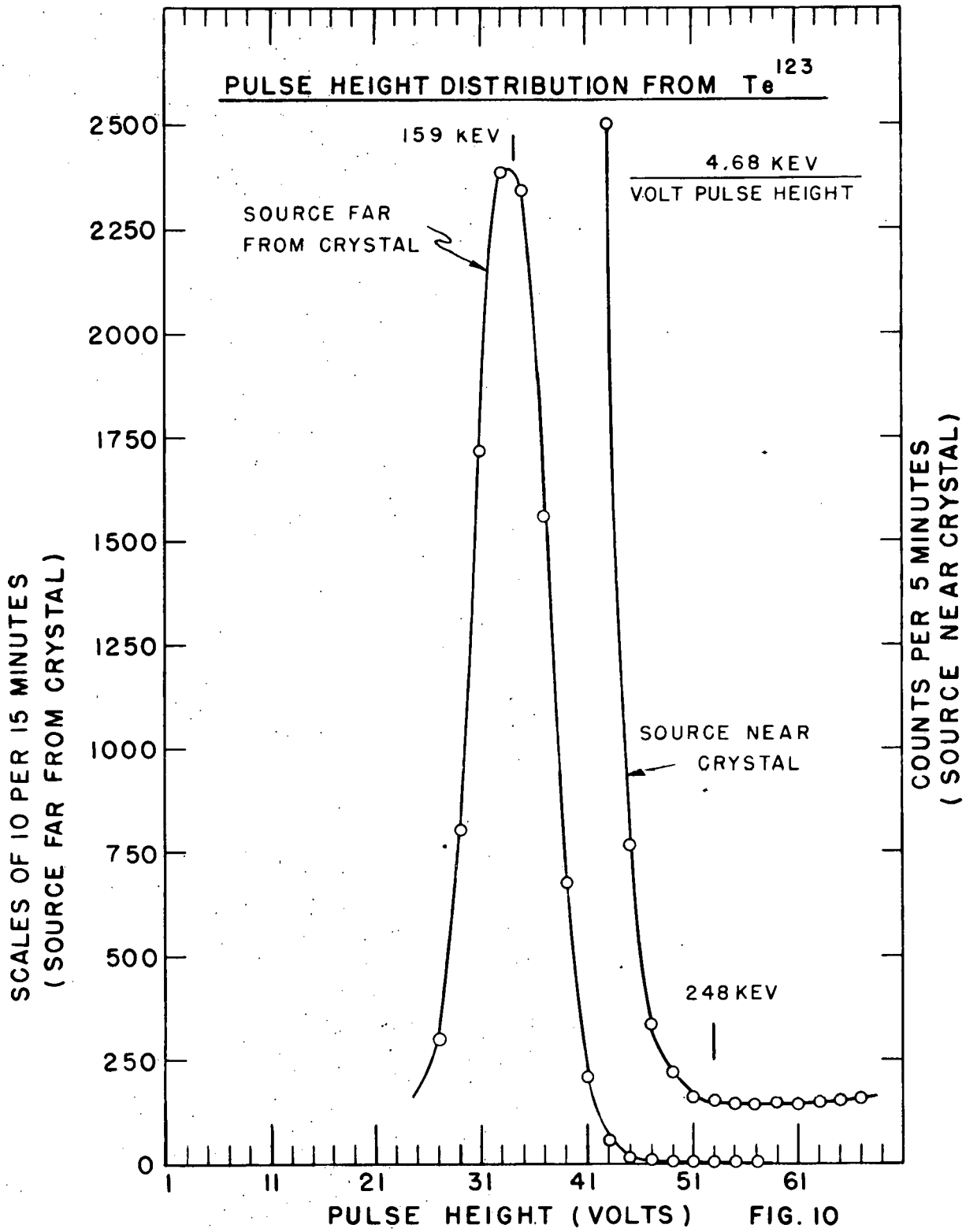

FIG. 10

DECLASSIFIED

observed data.

If the experimental counting rate at 53 volts was 3 standard deviations above its observed value, then one would say that the crossover had been observed. If one uses this value for the counting rate at the crossover energy, then a very high upper limit is found for the crossover. The experimental intensity ratio has to be corrected for absorption in the NaI, in the source and in the aluminum cap which surrounds the crystal. In addition, the intensities must be corrected for internal conversion. The tables[6] of Rose, et al were used to find α_K and the theoretical K/L ratios[2] were used to find α_L. The total α was assumed to be $\alpha_K + \alpha_L$.

The result of the above analysis is that the crossover ratio has a very conservative upper limit of 0.5%.

One possible reason for a value that is well below the 7% predicted by Weisskopf is that the theory is based on a single proton model. In the case of Te^{123}, an odd N nucleus, the theory may not be very good because of the lack of electric charge. Other examples[3] of this disagreement for odd N nuclei are found in the lifetimes of the E3 transitions. In addition, there may be effects due to cancellation of wave functions in the matrix element which could also give a smaller ratio.

6. M. E. Rose, G. H. Goertzel and C. L. Perry, ORNL 1023.

DECLASSIFIED

V. Results in Nuclear Spectroscopy (W. C. Rutledge)

1. 12-Minute $_{60}Nd^{151}$

A 12-minute activity produced by neutron bombardment of neodymium has previously been associated with Pm^{151}.[1] It has also been assumed that the parent Nd^{151} had a half-life too short to measure, as none was observed. The present investigation enables one to assign the 12-minute activity to Nd^{151}, and a newly discovered 27.5-hour daughter to Pm^{151}.

Enriched Nd^{150}, obtained from the Oak Ridge National Laboratory, was activated in the Argonne reactor. The internal conversion electrons and photo-electrons from a lead radiator were investigated in a permanent magnet-type-beta-spectrograph. Two gamma-rays of 85.4 and 117.1 kev, decaying with a half-life of 12 minutes, are characterized by conversion lines with work function differences of prometheum. In addition, K-X-rays of prometheum are observed by absorption in aluminum. Apparently these gamma-rays follow emission of the 12-minute 1.93 Mev beta-ray. A summary of the gamma-rays is given in the table below; no photo-electron lines were observed with this activity. A lead absorption curve of the beta-gamma coincidences resolves into two components - one gamma-ray of 990 kev, the other of about 150 kev. The latter is undoubtedly an unresolved mixture of the soft gamma-rays discussed above.

2. 27.5-Hour $_{61}Pm^{151}$

A 27.5-hour beta-ray, whose energy is measured by aluminum absorption as 1.1 Mev, is emitted from Pm^{151}. About 15 gamma-rays (tabulated below) are associated with this activity. The conversion lines from these gamma rays show work function differences of samarium. It is thus concluded that the 12-minute activity is the parent of the 27.5-hour

1. J. A. Marinsky, L. E. Glendenin, NNES 9, paper 194; B. H. Ketelle, ORNL May Quarterly Report, 1949.

DECLASSIFIED

daughter in Pm^{151}. This is the usual case where the half-lives of members of a chain with odd mass numbers increase successively down the chain. Aluminum absorption curves of beta-electron coincidences show the beta-ray to be in coincidence with conversion electron groups of 150 and 330 kev, which may be reasonably associated with gamma-rays of about 165 and 340 kev measured in the spectrograph. Aluminum absorption curves of gamma-electron coincidences show gamma-rays to be in coincidence with conversion electron groups of 40, 147, and 330 kev, which again may be associated with gamma-rays of about 65, 165, and 340 kev. Lead absorption curves of beta-gamma coincidences show the beta-ray to be in coincidence with the 340 kev gamma-ray. Further experiments are being conducted on this activity so as to make it possible to propose a decay scheme.

3. 15-Minute $_{42}Mo^{101}$ and 16-Minute $_{43}Tc^{101}$.

The gamma-rays associated with 15-minute Mo^{101} and 16-minute Tc^{101}, and previously reported in the quarterly report by internal conversion studies as 191.2 and 306.9 kev respectively, are confirmed by using lead and uranium as secondary radiators. This rules out the possibility of the 150 and 260 kev gamma-rays, reported in scintillation spectrometer studies,[2] as being unconverted and not observable by the present internal conversion techniques.

4. 3.5-Minute $_{34}Se^{79}$.

The gamma-ray of 95.9 kev associated in a previous quarterly report with a 16-minute half-life has been found to have a 3.5 minute half-life.

2. E. der Matoosian, Phys. Rev. 83, 223 (1951).

923 036

DECLASSIFIED

Radio-Isotope	Half Life	Mode of Decay	Electron Energy (Kev)	Proposed Interpretation	Energy Sum	Gamma-Ray Energy (Kev)
Nd^{151}	12 m	β-emission	40.2	K^1	85.4	85.4
			64.8	K^2	110.0	110.0
			71.9	K^3	117.1	117.1
			78.1	$L^1_{I,II}$	85.3	
			83.8	M^1	85.4	
			110.0	$L^3_{I,II}$	117.2	
			115.5	M^3	117.1	
				By lead absorption		990
Pm^{151}	27.5 h	β-emission	17.8	K^1	64.7	64.7
			18.9	K^2	65.8	65.8
			22.8	K^3	69.7	69.6
			32.6	Auger		
			37.4	Auger		
			53.1	K^4	100.0	99.9
			57.2	$L^1_{I,II}$	64.7	
			58.3	$L^2_{I,II}$(K)	65.8(105.2)	(105.0)
			61.9	$L^3_{I,II}$	69.4	
			63.1	M^1	64.8	
			64.1	M^2	65.8	
			69.2	K^5	116.1	116.2
			92.3	$L^4_{I,II}$	99.8	
			97.1	K^6(L)	144.0(104.6)	144.0
			103.2(weak)	(M)	(104.9)	
			109.0(weak)	$L^5_{I,II}$	116.5	

523 037

DECLASSIFIED

Radio-Isotope	Half Life	Mode of Decay	Electron Energy (Kev)	Proposed Interpretation	Energy Sum (Kev)	Gamma-Ray Energy (Kev)
			116.3	K^{7}	163.2	163.1
			121.1	K^{8}	168.0	168.0
			130.2	K^{9}	177.1	177.0
			136.4 (weak)	$L^{6}_{I,II}$	143.9	
			155.5	$L^{7}_{I,II}$	163.0	
			160.4	$L^{8}_{I,II}$	167.9	
			161.5	K^{10}	208.4	208.3
			169.4	$L^{9}_{I,II}$	176.9	
			174.9	M^{9}	176.6	
			185.0	K^{11}	231.9	231.9
			186.5	K^{13}(Pb)	274.8	
			192.8	K^{12}	239.7	239.9
			200.7	$L^{10}_{I,II}$	208.2	
			224.4	$L^{11}_{I,II}$	231.9	
			228.3	K^{13}	275.2	275.2
			232.6	$L^{12}_{I,II}$	240.1	
			251.7	K^{14}(Pb)	340.0	
			293.2	K^{14}	340.1	340.2
			324.0	L^{14}_{II} (Pb)	339.8	
			332.9	$L^{14}_{I,II}$	340.4	
				By lead absorption 615		
Mo^{101}	15 m β-emission		74.6	K(U)	191.0	By Conversion Electrons
			103.2	K(Pb)	191.5	191.2
			168.6	L(U)	190.0	
			175.9	L(Pb)	191.4	
Tc^{101}	16 m β-emission		190.7	K(U)	307.1	306.9

DECLASSIFIED

Radio-Isotope	Half Life	Mode of Decay	Electron Energy (Kev)	Proposed Interpretation	Energy Sum (Kev)	Gamma-Ray Energy (Kev)
			218.5	K(Pb)	306.8	
			290.8	L(Pb)	306.3	

In the study of the 27.5 hour Pm^{151}, a very weak gamma-ray of 121.8 kev with work function differences of samarium was attributed to 9-hour europium which decays by K-capture. There is a possibility that it is associated with Pm^{151}, but this could not be definitely established.

DECLASSIFIED

VI. Measurement of the Isomeric State of $_{21}Sc^{46}$ (20 Seconds)

(S. B. Burson and W. C. Rutledge)

The energy of a gamma-ray which is associated with the 20-second isomeric state of $_{21}Sc^{46}$ (reported by M. Goldhaber and C. O. Muehlhause, Phys. Rev. 74, 1877 (1948)) has been measured by spectrographic means. A semipermanent magnet type internal conversion electron spectrograph was used with the field set at 457 gauss. The vacuum lock of the camera chamber allowed the source to be inserted into position between 12 and 15 seconds after activation in the reactor. Eastman plates with a 25 micron N.T.B. emulsion were used. 85 successive activations and exposures produced two measurable lines tabulated below:

Electron Energy (Mev)	Proposed Interpretation	Energy Sum (Mev)	Gamma-Ray Energy (Mev)
0.1795	K	0.1840	0.184
0.1836	L	0.1841	

E. der Mateosian and M. Goldhaber (Phys. Rev. 82, 115 (1951)), on the basis of measurements made with a scintillation spectrometer, have assigned an energy of 0.135 Mev to what is presumably this same gamma ray. Our higher value of 0.184 Mev brings the point for this isomer on a lifetime-energy plot into even better agreement with the 1 ⇌ 3 group than is indicated by M. Goldhaber and A. Sunyar in a report to be published later.

023 040

DECLASSIFIED

VII. Product Compounds Formed by Recoil Iodine Atoms in Dilute Solutions of Ethyl Iodide in Benzene and Iodine in Benzene (Frances Mohr and S. Wexler)

A. Introduction

Almost from the discovery of neutron activation, interest has been shown in the reactions undergone by the energetic recoils resulting from the emission of gamma-rays.[1,2] More recently, identification of the products formed by halogen recoils in organic solvents has been used to test the liquid cage theory of activity retention.[3,4] In this theory, the reactions in the liquid phase produced by atoms formed in the n, γ process are described in terms of slowing down by elastic collisions, dissociation of solvent molecules, and eventual reaction of the molecular fragments and the free atoms in a liquid cage.[5,6] In this report we present the first results of our study of products formed by I^{128} recoils in benzene solution. The high neutron flux available from CP-3' has made possible investigations using very dilute solutions of iodine and ethyl iodide. To the irradiated solutions appropriate organic iodide carriers were added and the mixtures were fractionally distilled. CH_3I^{128}, $C_2H_5I^{128}$ and $C_6H_5I^{128}$ were found in the collected fractions.

B. Materials and Procedure

Reagent grade benzene was stored over sodium for about two weeks and then distilled from the sodium. The carriers methyl iodide, ethyl iodide and phenyl iodide were each distilled through a packed glass column. Middle fractions were taken. The reagent grade iodine was used without further purification.

A 15 ml aliquot of the dilute solutions of C_2H_5I or I_2 in C_6H_6 was irradiated near the reflector of the "goat hole" for thirty minutes in a

1. E. Gluckauf and F. W. Fay, J. Chem. Soc. 390 (1936).
2. W. F. Libby, J. Amer. Chem. Soc. 62, 1930 (1940).
3. L. Friedman and W. F. Libby, J. Chem. Phys. 17, 647 (1949).
4. J. M. Miller and R. W. Dodson, J. Chem. Phys. 18, 865 (1950).
5. W. F. Libby, J. Amer. Chem. Soc. 69, 2523 (1947).
6. J. M. Miller, J. W. Gryder and R. W. Dodson, J. Chem. Phys. 18, 579 (1950).

DECLASSIFIED

flux of 10^{11}n/sec/cm^2. The irradiated solution was transferred to a separatory funnel, 5 ml of benzene containing molecular I_2 and 20-30 ml of each organic iodide were added as carriers and the solution was then extracted with 0.06 M $NaHSO_3$ solution. The irradiating tube made of boron-free glass and the standard taper stopper were also rinsed with the bisulfite solution. The organic phase was then fractionally distilled through a three foot packed glass column. In the first group of experiments a middle fraction of approximately 15 ml of each carrier was collected. Later, 3 ml fractions were taken continuously. The gamma activities in the distillates and in the aqueous phase were measured in a high pressure ionization chamber. The half-life of each sample was followed to assess radiochemical purity. The activity was corrected for decay and for the volume distilled. From the total 25 min I^{128} activity measured in each experiment the percentage of activity in each collected portion was calculated.

C. Results and Discussion

The data from the "middle fraction" experiments (Table V) demonstrates the formation of $C_2H_5I^{128}$ and $C_6H_5I^{128}$ following radiative capture of neutrons by I^{127} present either as molecular iodine or as ethyl iodide in the benzene solutions. Although the percent of radio-phenyl iodide formed seems not to depend on the target iodine molecule, the fraction of the activity appearing as $C_2H_5I^{128}$ is considerably higher when inactive ethyl iodide is irradiated. This remains true when molecular iodine in a concentration low relative to that of ethyl iodide is added to react with any impurities present in the reagents (Exp. 6 and 7, Table V). Thus, it appears that reaction of the recoils with impurities is not a likely cause of the presence of radio-ethyl iodide among the products.

However, the finding of I^{128} activity in the benzene fraction suggested the presence of products other than ethyl and phenyl iodide so a more thorough investigation of the distribution of activity in the distillate was performed.

DECLASSIFIED 523 042

TABLE V

Percent of I^{128} Activity in Distilled Fractions

Exp.	Mole Fraction Irradiated I Compound		Percent of Total I^{128} in Various Fractions		
	I_2	C_2H_5I	C_2H_5I	C_6H_6	C_6H_5I
1		3.4×10^{-3}	7.7	4.3	12.4
2		3.4×10^{-3}	8.2	6.5	16.5
3	3.4×10^{-3}		<1	<1	11.9
4	3.4×10^{-3}		1.1	1.7	11.2
5	3.4×10^{-3}		1.5	1.5	14.4
6	1.7×10^{-4}	3.2×10^{-3}	4.7	3.2	12.7
7	1.7×10^{-4}	3.2×10^{-3}	6.1	2.9	13.3

TABLE VI

Normal Boiling Points of Added Carriers

Carrier	B. P. (°C.)
Methyl Iodide	42.5
Ethyl Iodide	68
Benzene	80
Iodobenzene	182

The distillate was collected in a continuous series of 3 ml fractions. A preliminary experiment in which a solution of I_2 in benzene was irradiated and no organic iodide carriers were added showed the presence of two active iodine fractions, one distilling with the first several 3 ml benzene distillates and the greater part remaining in the pot after collection of seventeen 3 ml benzene portions. This was followed by runs in which organic iodide carriers were present during distillation. The boiling points of the carrier compounds of interest are given in Table VI. The percent of

DECLASSIFIED

I^{128} in each fraction, corrected to exactly 3 ml of volume, is arranged in Table VII adjacent to the temperature at the head of the column during the period of collection. In Exp. 1 molecular I_2 was the target; C_2H_5I and C_6H_5I were the added carriers. The constancy of the percentage figures (i.e. the specific activity of I^{128}) in the temperature region of 68-72° C. and at 182° C. again demonstrates the formation of radio-ethyl and radio-phenyl iodides. The higher percent of activity in the first collected portion suggests the presence of CH_3I^{128} among the products, and in Exp. 2 methyl iodide was included among the carriers. The relatively constant specific activities of the fractions boiling at 42° C. makes the presence of active methyl iodide likely. Ethyl iodide was the principal iodine target in Exp. 3. In the distillate one finds CH_3I^{128}, $C_2H_5I^{128}$ and $C_6H_5I^{128}$. Comparing the specific activities of the corresponding fractions for the three experiments, one sees that the percent of radio-iodine in each of the lower boiling portions is higher in the irradiated C_2H_5I-benzene solution than in the I_2-benzene solutions. This is particularly true of the ethyl iodide fractions boiling in the range 66-72° C. The presence of I^{128} activity in distillates boiling at temperatures between those of pure ethyl iodide and benzene is disturbing, but may be due to inability of the distilling column to resolve the two completely. This is indicated by the slow rise of boiling temperature between 70° and 80°, accompanied by a decrease in specific activity of the collected fractions. Nevertheless, this region is being investigated more thoroughly.

Finding of active methyl, ethyl and phenyl iodides as products in the reactions of recoil I^{128} atoms throws some light on the mechanism of the reactions. In the liquid cage model an energetic iodine atom, initially with energy of a few hundred electron volts, is slowed down

DECLASSIFIED

TABLE VII

Variation of I^{128} in Collected Fractions as Function of Distillation Temperature

Exp. 1 Mole fraction of $I_2 = 3.4 \times 10^{-3}$		Exp. 2 Mole fraction of $I_2 = 3.4 \times 10^{-3}$		Exp. 3 Mole fraction of $I_2 = 1.8 \times 10^{-4}$, $C_2H_5I = 6.5 \times 10^{-3}$	
Temp. Range (°C.)	% I^{128} in 3 ml Distillate	Temp. Range (°C.)	% I^{128} in 3 ml Distillate	Temp. Range (°C.)	% I^{128} in 3 ml Distillate
65-72	0.4	41	0.06	31-43	0.2
72	0.2	42	0.08	43	0.2
72	0.1	42	0.08	43	0.3
68-72	0.1	42	0.09	43-45	0.3
68	0.1	42-44	0.1	45-55	0.5
68	0.1	44-57	0.2	55-65	0.9
68-69	0.1	58-68	0.2	66-70	1.1
69-70	0.2	68-72	0.08	71-72	1.1
75-78	0.5	72	0.02	72-73	1.0
78	0.3	72-73	0.01	73	0.9
78	0	74	0	74	0.9
179	1.4	74	0	74	0.9
182	1.5	74-75	0	75-76	0.8
182	1.5	75	0.01	76-77	0.8
182	1.5	75	0	77-78	0.7
182	1.4	75-76	0.08	78-79	0.6
		76-77	0.08	79	0.2
		77-78	0	79-178	0
		77-78	0	182	0.8
		78-80	0	182	1.0
		80-100	0	182	1.2
		179-182	0.9	182	1.2
		182	0.9	182	1.1
		182	0.8	182	1.3
		182	0.9	182	1.2
		182	0.9	182	1.4
		182	0.8		
		182	0.8		
		182	0.9		

by collisions with benzene molecules. Eventually, the recoil is slowed down sufficiently so that it lacks the energy necessary to escape from the particular liquid cage of benzene molecules in which it happens to be present. The I^{128} then combines with fragments of benzene molecules resulting from previous collisions which are in the same cage. According to this picture, the presence of CH_3I^{128} and $C_2H_5I^{128}$ among the products suggests

DECLASSIFIED

that a benzene molecule may be largely shattered in a collision with an energetic iodine atom. Further, since the activity of the $C_2H_5I^{128}$ is greater when ethyl iodide is the target than for I_2 either some part of the energetic recoils recombine with the ethyl radicals from the initial rupture of the bond following radiative capture, or energetic I^{128} atoms may exchange with an inactive ethyl iodide molecule during the slowing down period.

923 046

DECLASSIFIED

VIII. Yield and Fraction of Positive Gold Recoil Atoms (S. Yosim)

Work has been continued on the yield of radioactive gold recoil atoms and the fraction of them that is positively charged. The effect on this fraction of varying the applied positive voltage is shown in the following table.

Chamber	2 x Y (%)**	% Positive Recoils	Voltage
51	72.6		
52*	70.8	59.6	1500
54	34.2	48.8	1500
55	64.0		
58	45.2	61.8	1500
59	19.2(?)		
60	44.4	50.0	22½
61*	71.2	61.2	92

*Film prepared and irradiated without exposure to the atmosphere.

**Y = number of recoils collected divided by the number of recoils created in an ideal top layer of source.

The values of chambers 60 and 61 are only approximate, as the decay curves must still be followed. However, it is interesting to note that the effect of a retarding field is marked even for only 22.5 volts applied. This does not necessarily imply that the energy of the recoil atom is less than 22.5 volts. One must remember that because of the Auger effect, the charge on the recoil atom is likely to be greater than one electronic charge. Further, these experiments in which the applied voltage is varied indicate the Ve of the free recoil ion in space but says nothing of the initial Ve immediately following the emission of the capture γ-rays. We shall continue the work by applying still lower potentials to see, if possible, where the voltage effect ends.

923 047

DECLASSIFIED

IX. Conversion Electrons from Capture γ-Rays in Gold (S. Yosim)

The existence of soft internal conversion electrons associated with neutron capture γ-rays has been shown for a variety of nuclei by various methods.[1-3]

In order to test the hypothesis that the positive charges found on approximately 60% of recoiling gold and indium atoms are formed as a result of such internal conversion of capture γ-rays, it was desirable to demonstrate the presence of the conversion electrons with gold.

A method previously applied by Muehlhause was used. This involved covering with an X-ray film a thin gold foil (10 mg/cm^2) mounted on lucite, placing this in a hollow bismuth box and exposing the entire system to the thermal beam of GP-3'. In order to differentiate between the internal conversion effect and secondary effects such as the photoelectric and Compton effects, lead absorbers were placed between the gold foil and the film. If the darkening were due to internal conversion only, the lead would be a very effective absorber since its neutron capture cross section is low. However, if the darkening of the film were due solely to the secondary effects, the lead would act as a source and would be indistinguishable from the gold since the atomic numbers are approximately the same.

In one experiment, half of the lucite was covered with gold. On each half, lead and aluminum foils of various thicknesses were placed. Examination of the film showed that some blackening was produced by the lead which was directly on the lucite. However, the blackening due to the gold was more intense. This indicates that while the secondary effect is present, the dominating one is that of internal conversion. A film which was exposed to the radioactive gold for an equivalent time was blank. This eliminates the possibility of the beta particles from Au^{198} causing the blackening. Aluminum absorbers indicate that the radiations are quite soft. We expect to measure the half thickness and range of the radiation by use of a densitometer.

1. Hoffman and Bacher, Phys. Rev. 54, 644 (1932).
2. Amaldi and Rasetti, Ricerca Sci. 10, 115 (1939).
3. Muehlhause and Hibdon, Abstract, Washington Meeting, Am. Phys. Soc., April 1951.

UNCLASSIFIED

Mass Spectroscopy

X. Reports by Mark G. Inghram

1. Fission Yields (Ellis Steinberg, L. E. Glendenin, D. C. Hess, Mark G. Inghram)

In the previous quarterly report (ANL-4659) the fission yields of the zirconium isotopes in a 5.3 year old zirconium sample were given. We have now measured the molybdenum isotopes from the same sample. The results are given in Table VIII.

Table VIII

Yields of Zirconium and Molybdenum Isotopes from U^{235} Fission

Element	Mass Number	Fission Yield	Element	Mass Number	Fission Yield
Zr	90	5.02	Mo	95	6.25*
	91	5.49		97	5.93
	92	5.62		98	5.90
	93	6.02		100	6.46
	94	6.20*			
	95	6.15			

* Normalized to the smooth radiochemical fission yield curve at these points.

A plot of these yields shows a peak of 25 per cent at mass 100 which does not appear on the radiochemical curve. This peak corresponds to the peak observed in xenon at mass 134 by Thode. It is tempting to explain these fine structure peaks as due to closed shells in the primary fission nucleus, i. e., at Te^{134}_{82}. To check this hypothesis further, we have extracted zirconium and molybdenum from the fission of U^{233}. Only preliminary calculations

DECLASSIFIED

have been made; the necessary corrections for multiplier discriminations, etc., have not yet been made. There is, therefore, no point in quoting values normalized to the radiochemically determined fission yield curve. Table II gives the rough preliminary data.

Table II.

Yields of Zirconium and Molybdenum Isotopes from U^{233} Fission

Element	Mass Number	Relative Fission Yields	Element	Mass Number	Fission Yield
Zr	91	1.1	Mo	95	1.2
	92	1.2		96	.01
	93	1.2		97	≡ 1.0
	94	1.1		98	1.0
	96	≡ 1.0		100	.7

Plots of these data show an excess in the 98 and 100 position over that expected. The yield at mass 96 is a case of direct yield of Nb^{96} fission.

From the practical standpoint it is apparent that the use of Tc^{99} as a measure of the amount of fission can lead to ambiguous results. This isotope does not lie on the smooth fission yield curve in either U^{235} or U^{233} fission, hence assuming the smooth fission yield gives a measure of fission which is too high.

2. Double Beta Radioactive Decay (R. J. Hayden, M. G. Inghram)

A search for an example of double beta radioactive decay has been made by extracting the daughter element from geologically old minerals and looking for an isotopic excess due to the decay process. Previous results

DECLASSIFIED

have indicated the possibility of double beta decay in the case of xenon extracted from 1.5×10^9 years old Bi_2Te_3. The particular process in question is

$$Te^{130} \longrightarrow Xe^{130} + 2\beta.$$

The results, however, were seriously complicated by the relatively large amounts of Xe^{129} and Xe^{131} found in the samples investigated. It was postulated that these excesses were due to neutron absorption in Te^{128} and Te^{130}. In order to test this hypothesis we have investigated the xenon from an andalusite-sericite rock containing Bi_2Te_3. This rock should have a much lower uranium content than rutile which was the rock used in our earlier investigation. The results indicate that the excess isotopes at Xe^{129} and Xe^{130} do not result from a spontaneous process in tellurium, but are of secondary origin. The previous explanation of neutron absorption still appears the most tenable. The excess peak at mass 130 is such as to indicate a half-life for double beta decay somewhat longer than our previous value of 1.5×10^{21} years. This increase brings the half-life into closer agreement with the half-life predicted from the Dirac theory of the neutrino.

3. Dissociation Energies of Alkali Halide Molecule-Ions (W. A. Chupka)

Early studies of ion emission from hot salts have been concerned mostly with the identification of the ions emitted, the determination of the relative amounts of both positive and negative ions and the variation of emission with time, temperature, and concentration of impurities[1,2]. A few studies of thermodynamic equilibria among gaseous ions of salts have been reported, such as those of Helmoholtz and Mayer[3] in their experimental

DECLASSIFIED

measurements of lattice energies of some alkali halides. More recently complex ions of the type $NaKCl^+$ have been observed in the mass spectrometer.[4] The purpose of the present experiment was to study the ion emission from alkali halides and to determine the binding energy of these complex ions by measuring the equilibrium constants for their dissociation at a series of temperatures.

Most of the present investigation was restricted to complex ions of the type M_2X^+ emitted from the pure alkali halide MX. The equilibrium constant for the following reaction was measured at a series of temperatures.

$$(1) \qquad M_2X^+_{(g)} \longrightarrow M^+_{(g)} + MX_{(g)}$$

The slope of a plot of $\ln K_e$, the natural logarithm of the equilibrium constant, versus $1/T$, where T is the absolute temperature, gives the change in heat content, ΔH, for the reaction from the equation

$$(2) \qquad \frac{d \ln K_e}{d\,(1/T)} = -\frac{\Delta H}{R}$$

The ΔH for the reaction is also calculated by estimating the change in entropy, ΔS^o, for the reaction and using the equation

$$(3) \qquad \Delta H^o = \Delta F^o + T\Delta S^o$$
$$= -RT \ln K_e + T\Delta S^o$$

where the superscripts indicate that the substances are in their standard states which will be chosen as the gases at one atmosphere of pressure. The change in heat content at absolute zero, $\Delta H(0^oK)$, is then obtained by subtracting from $\Delta H(T^oK)$ the difference of the quantities $(H-H_o)$ for

DECLASSIFIED

products and reactants, where $(H-H_o)$ is the difference in heat content of the substance at T^o K and at 0° K.

The method of measuring the equilibrium constant consisted of measuring the ratio M^+/M_2X^+ for ions emitted through a slit in an oven containing the alkali halide. This ratio, together with the vapor pressure of the alkali halide which is assumed to be that of the pure alkali halide at the temperature of the oven, gives the equilibrium constant.

Measurements have been made on four salts. Typical ion ratios are recorded in Table IX. Since M^+/M_2X^+ is the equilibrium constant for the reaction

$$(4) \qquad M_2X^+_{(g)} \longrightarrow MX_{(crystal)} + M^+_{(g)}$$

the data should obey the equation

$$(5) \quad \log_{10} \frac{M^+}{M_2X^+} = C - A\left(\frac{1000}{T}\right) - \frac{3}{2}\log_{10}\left(\frac{1000}{T}\right)$$

The last term in this expression results from the assumption that

$$(6) \quad C_p(\text{Products}) - C_p(\text{Reactants}) = \frac{3}{2} R.$$

The constants A and C were evaluated from the temperature plots. Values of $\Delta H_1(800^o\ K)$ for the reaction given by equation (4) were obtained from equation (5) by means of the relation

$$(7) \qquad \frac{d \ln (M^+/M_2X^+}{d\,(1/T)} = -\frac{\Delta H}{R}$$

the ΔH for the reaction given in equation (1) was then obtained by adding the ΔH of vaporization of MX. This value can be corrected to ΔH at 0° C by subtracting the difference of the quantity $(H - H_o)$ for products and

DECLASSIFIED

Table IX

KCl		KBr	
$\log_{10}\frac{K^+}{K_2Cl^+}$	$\frac{1000}{T}$ (°K)	$\log_{10}\frac{K^+}{K_2Br^+}$	$\frac{1000}{T}$ (°K)
.210	1.399	.955	1.376
.177	1.376	.910	1.354
.128	1.354	.846	1.333
.114	1.333	.792	1.312
.056	1.312	.712	1.293
.007	1.293	.663	1.272
- .022	1.272	.585	1.254
- .102	1.236	.536	1.236
		.452	1.201

reactants. This correction can be calculated by standard methods.

A second method of calculating the heats of reaction is as follows. The equilibrium constant at 800° C is determined from equation (5) (correcting by a factor to give the ratio of the total concentrations of M^+ and M_2X^+) together with the value of the value of the vapor pressure of MX taken from the literature. The value of ΔS^o, the change in entropy of the reaction for the substances in their standard states is calculated by standard methods and used in equation (3) to obtain ΔH^o at 800°-K. The various quantities calculated are summarized in Table X.

DECLASSIFIED

Table X

Ion	ΔH^o (Theoretical) 800°K in K cal/mole Entropy Calculation	ΔH^o (Dissociation) 800°K in K cal/mole Experimental values
Na_2Cl^+	46	42 ± 3
K_2Cl^+	43	41 ± 3
K_2Br^+	40	37 ± 4
Rb_2Cl^+	41	40 ± 5

The agreement of the measured values, though they can be considered as only preliminary, with theoretical values gives confidence in the applicability of the method.

1. O. W. Richardson, "The Emission of Electricity from Hot Bodies", Longmans, Green and Co., London, 1st ed. 1916, pp. 234-82.
2. A. L. Reimann, "Thermionic Emission", John Wiley and Sons, Inc., New York, 1934, pp. 273-85.
3. Helmholtz and J. E. Mayer, J. Chem.Phys., 2, 245 (1934).
4. R. J. Hayden, Phys. Rev. 74, 651 (1948).

4. Argon Geological Age Method (R. J. Hayden, M. G. Inghram)

The argon age of Essonville Granite has been determined as 0.6×10^9 years. The geological age of this granite is known from uranium-lead data quoted in the previous quarterly report (ANL-4659) to be of the order of $1. \times 10^9$ years. This low result points out that argon ages even on such crystaline rocks as granites are definitely in error; the degree of error varying with the degree of alteration of the rock or mineral.

DECLASSIFIED

Thus argon ages can be taken as only a lower limit of geological age and probable ages extrapolated from the apparent age will require a great deal of experimental calibration.

523 656

DECLASSIFIED

Theoretical Physics

XI. Threshold Values of Internal Conversion Coefficients for the K-Shell (B. I. Spinrad and L. B. Keller)

Recent computations of the internal conversion coefficients for the K-shell have been reported for various Z and for k (γ-ray energy) greater than 0.3-0.5 electron masses.[1] The extrapolation of these results to lower energies is uncertain for two reasons: first, the mathematical formulation of the problem is of such complexity that no simple extrapolation rule can be used; second, the numbers are computed for unscreened wave functions.

In an attempt to resolve the mathematical difficulties, computations have been made on the threshold values of the conversion coefficients. These computations were performed by taking the limiting values of the formulae of reference (1) as p, the electron momentum, approaches zero positively. Under these conditions, many simplifications arise, and it is possible to compute the results on a desk machine.

The results are tabulated in the table following. The notation is that of reference (1). Since screening has been ignored, the threshold energies for which these results were computed were those obtained from the relativistic single electron model, given by $k = 1 - (1 - [\alpha Z]^2)^{\frac{1}{2}}$. Figures in parentheses indicate the power of 10 by which the number must be multiplied.

---

1. Rose, Goertzel, Spinrad, Harr, and Strong, Phys. Rev. 83, 79 (1951).

823 057

DECLASSIFIED

Threshold Values of Internal Conversion Coefficients for the K-Shell

(The number in parentheses is the power of 10 by which the corresponding numbers are to be multiplied)

Z	α_1	α_2	α_3	α_4	α_5	β_1	β_2	β_3	β_4	β_5
10	$7.329^{(3)}$	$8.184^{(5)}$	$4.281^{(7)}$	$1.340^{(9)}$	$2.867^{(10)}$	$4.222^{(2)}$	$2.219^{(5)}$	$3.472^{(7)}$	$2.587^{(9)}$	$1.124^{(11)}$
20	$4.510^{(2)}$	$1.251^{(4)}$	$1.596^{(5)}$	$1.232^{(6)}$	$6.459^{(6)}$	$1.087^{(2)}$	$1.415^{(4)}$	$5.471^{(5)}$	$9.874^{(6)}$	$1.084^{(8)}$
30	$8.720^{(1)}$	$1.030^{(3)}$	$6.060^{(3)}$	$1.922^{(4)}$	$4.338^{(4)}$	$5.075^{(1)}$	$2.893^{(3)}$	$4.867^{(4)}$	$3.919^{(5)}$	$1.841^{(6)}$
40	$2.403^{(1)}$	$1.606^{(2)}$	$5.600^{(2)}$	$9.300^{(2)}$	$1.123^{(3)}$	$3.072^{(1)}$	$8.942^{(2)}$	$8.830^{(3)}$	$3.892^{(4)}$	$1.003^{(5)}$
50	$1.085^{(1)}$	$3.741^{(1)}$	$8.317^{(1)}$	$8.112^{(1)}$	$5.926^{(1)}$	$2.123^{(1)}$	$3.881^{(2)}$	$2.374^{(3)}$	$6.466^{(3)}$	$1.032^{(4)}$
60	$5.190^{(0)}$	$1.081^{(1)}$	$1.623^{(1)}$	$1.035^{(1)}$	$4.834^{(0)}$	$1.737^{(1)}$	$2.033^{(2)}$	$8.215^{(2)}$	$1.484^{(3)}$	$1.626^{(3)}$
70	$2.713^{(0)}$	$3.604^{(0)}$	$3.721^{(0)}$	$1.598^{(0)}$	$5.479^{(-1)}$	$1.548^{(1)}$	$1.225^{(2)}$	$3.393^{(2)}$	$4.257^{(2)}$	$3.158^{(2)}$
80	$1.636^{(0)}$	$1.334^{(0)}$	$9.516^{(-1)}$	$3.152^{(-1)}$	$8.995^{(-2)}$	$1.528^{(1)}$	$8.304^{(1)}$	$1.605^{(2)}$	$1.436^{(2)}$	$7.637^{(1)}$
88	$9.989^{(-1)}$	$6.622^{(-1)}$	$3.551^{(-1)}$	$1.094^{(-1)}$	$2.977^{(-2)}$	$1.764^{(1)}$	$6.582^{(1)}$	$9.549^{(1)}$	$6.576^{(1)}$	$2.714^{(1)}$
96	$6.691^{(-1)}$	$3.661^{(-1)}$	$1.848^{(-1)}$	$4.991^{(-2)}$	$8.452^{(-3)}$	$2.313^{(1)}$	$5.608^{(1)}$	$6.060^{(1)}$	$3.394^{(1)}$	$1.034^{(1)}$

523 058

XII. Thermodynamic Functions on the Generalized Fermi-Thomas Theory

(Malcolm K. Brachman)

Recently, equations of state of the elements[1] based on the generalized Fermi-Thomas theory have been developed. It has been shown[2] that exchange effects may be neglected for high temperatures, and they will not be considered here. In the past, the pressure has been obtained by calculating the rate of flow of momentum through the surface of the atom, which is assumed to be a sphere of radius a. It is also possible to find the pressure from the free energy or the logarithm of the partition function.[3] The purpose of this note is to show that the pressure calculated from the free energy using the generalized Fermi-Thomas model for arbitrary temperatures agrees with that found by mechanical considerations based on the same model, and, in addition, one obtains expressions for the entropy and the specific heat.

Our model leads to the kinetic energy density[4]

$$E_K(r) = \frac{4\pi}{h^3} (2\,m)^{3/2} \beta^{-5/2} I_{3/2} (\eta + \beta e V(r)) \tag{1a}$$

and the electron number density

$$\rho(r) = \frac{4\pi}{h^3} (2\,m)^{3/2} \beta^{-3/2} I_{1/2} (\eta + \beta e V(r)), \tag{1b}$$

where $V(r)$ is the total potential, $V_N + V_e$, and $\beta = (kT)^{-1}$. Here V_N is the nuclear potential $\frac{Ze}{r}$, and $-V_e$ satisfies Poisson's equation with the charge density $e\rho(r) = \rho_e$. The boundary conditions are the vanishing of the total potential and the electric field at the surface of the atom. The volume integral of (1a) is the kinetic energy E_{kin} and that of (1b) is Z, the nuclear charge. The potential energy E_{pot} is

$$E_{pot} = -\tfrac{1}{2} \int_0^a \rho_e V_e \, d\tau - \int_0^a \rho_e V_N \, d\tau = E_{e,e} + E_{e,N} , \tag{2}$$

1. R. P. Feynman, N. Metropolis, and E. Teller, Phys. Rev. 75, 1561 (1949).
2. H. Jensen, Zeits. f. Physik 111, 373 (1938).
3. R. E. Marshak, P. M. Morse, and H. York, Ap. J. 111, 214 (1950).
4. The notation is the same as that of reference 1, except that our $\rho = -\rho_e$ of it.

523 059

DECLASSIFIED

where $d\tau$ is $4\pi r^2 dr$. By mathematical manipulation, one finds the virial theorem

$$E_{kin} = \frac{3}{2} p v - \frac{1}{2} E_{pot}. \tag{3}$$

The difference between our calculation and previous ones is that the pressure is obtained by macroscopic rather than microscopic considerations.

The pressure p and the entropy S are found from the free energy $F = E_{tot} - TS$, where T is the absolute temperature, by means of the thermodynamic relations

$$p = -\left(\frac{\partial F}{\partial v}\right)_T, \tag{4a}$$

$$S = -\left(\frac{\partial F}{\partial T}\right)_v . \tag{4b}$$

The basis of our work is the Gibbs-Helmholtz equation in the form

$$E_{tot} = \frac{\partial}{\partial \beta} \left[\beta F\right], \tag{5}$$

of which we obtain the indefinite integral. This is done by integrating the various terms of E_{tot} by parts and using the relations between the derivatives of $E_K(r)$ and ρ_e obtained by differentiating (1a) with respect to a, β, and r, including the cross derivatives. Employing Green's theorem, one finds

$$F = -\frac{2}{3} E_{kin} - E_{e,e} + ZkT\eta \tag{6}$$

From the relations (4a) and (4b) it follows that

$$p = \frac{2}{3} E_K(a), \tag{7a}$$

$$S = T^{-1} \left\{ \frac{5}{3} E_{kin} + 2 E_{e,e} + E_{e,N} \right\} - Zk\eta \tag{7b}$$

The first of these is the value obtained from mechanical considerations. The second in conjunction with the virial theorem yields Fermi's relation

$$E_{e,N} = -7 E_{e,e}, \tag{8}$$

in the limit as TS tends to zero.

DECLASSIFIED

The specific heat at constant volume, C_v, given by the relation

$$C_v = - \beta \left(\frac{\partial S}{\partial \beta}\right)_v , \tag{9}$$

may be expressed in the form

$$\frac{4}{3} TC_v = 5 p v + \frac{7}{6} E_{e,e} + \frac{1}{6} E_{e,N} - Ze\beta \frac{\partial V_e(0)}{\partial \beta} - Z \frac{\partial \eta}{\partial \beta} - \upsilon \rho(a) \frac{\partial \eta}{\partial \beta} \tag{10}$$

This differs from that given in reference 1.

523 061

DECLASSIFIED

XIII. Alphas and Gammas from the Proton Bombardment of Be^9 (D. R. Inglis and R. E. Malm)

In the proton bombardment of Be^9, resonances have been observed[1] in the yield of alphas, gammas, deuterons, neutrons, and scattered protons. The only known resonance above about 1 Mev is at 2.6 Mev and has been observed[2] for both gammas and neutrons, the latter in the reaction yielding B^9 plus protons, or perhaps Be^8 plus neutrons plus protons. The gammas have been attributed[1] to the reaction $Be^9(p,\alpha)Li^{6*}(\gamma)Li^6$, and if this were the case the same resonance would be observed in the low-energy alphas of this reaction. Preliminary observations have been made of these alphas and the gammas from a Be target about 10^{-4} cm thick without backing. The two groups of alphas, corresponding to the ground state and the 2.19 Mev excited state[3] of Li^6, were observed in a 16 inch, two-dimensional focussing magnetic spectrometer which has recently been put in operation in connection with the Argonne statitron. The varying yield of product particles, observed in a proportional counter, as the magnetic field was varied, is shown in Fig.11(a). The peaks correspond to both groups of alphas and to protons scattered elastically from Be, C, and O. The gammas were observed with a NaI crystal, no attempt being made at energy discrimination. The proton energy was varied through a small range near the expected resonance, and the resonance was observed for the gammas as previously reported,[2] but not for either group of alphas, as shown in Fig.11(b). This means that the resonant gammas are not associated with the 2.19 Mev state of Li^6. By the rough absorption technique, their energy has been estimated[2] as about 3.0 Mev if they are monochromatic. This could be a rough average energy if they are not monochromatic. It is suggested that the gammas are

1. Hornyak, Lauritzen, Morrison, and Fowler, Rev. Mod. Phys. 22, 291 (1950). This contains further references.
2. W. J. Hushley, Phys. Rev. 67, 34 (1945).
3. Browne, Williamson, Craig, and Donahue, Phys. Rev. 83, 179 (1951).

DECLASSIFIED

the result of cascade emission after simple proton capture, perhaps about as indicated by the broken lines in[4] Fig.11(c), though doubtless with some greater complexity.

4. F. Ajzenberg, Phys. Rev. 82, 43 (1951).

523 063

DECLASSIFIED

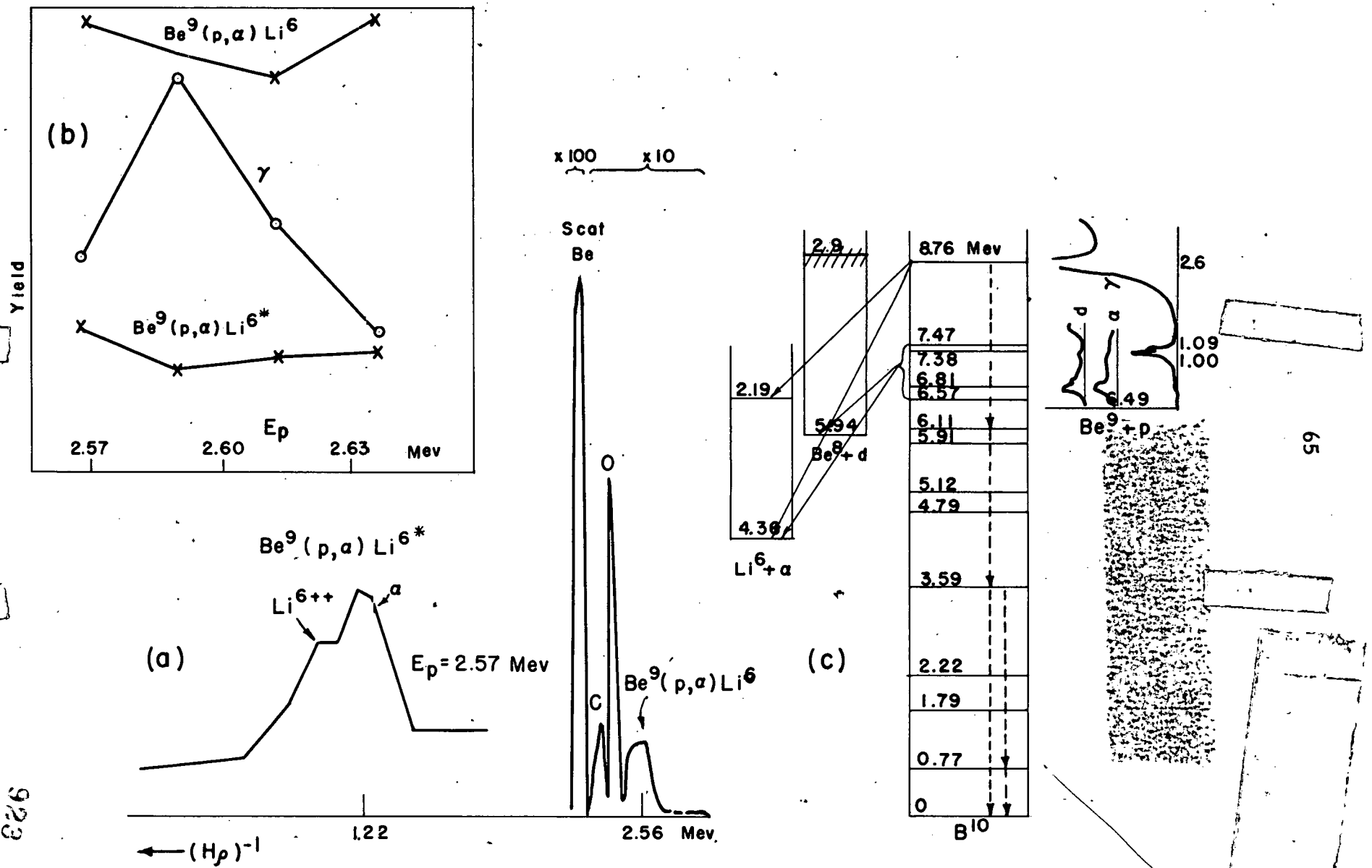
(b)
Yield
$Be^9(p,\alpha)Li^6$
γ
$Be^9(p,\alpha)Li^{6*}$
E_p
2.57
2.60
2.63
Mev
(a)
$Be^9(p,\alpha)Li^{6*}$
Li^{6++}
α
$E_p = 2.57$ Mev
1.22
$(H\rho)^{-1}$
x 100
x 10
Scat
Be
O
C
$Be^9(p,\alpha)Li^6$
2.56 Mev
(c)
2.19
4.36
$Li^6+\alpha$
2.9
5.94
Be^8+d
8.76 Mev
7.47
7.38
6.81
6.57
6.11
5.9
5.12
4.79
3.59
2.22
1.79
0.77
0
B^{10}
2.6
d
γ
α
1.09
1.00
6.49
Be^9+p

FIG. 11